Computational Neuroscience for the Clinic :

Transcranial stimulation for Parkinson's Disease

Erin Beate Bjørkeli

Thesis submitted for the degree of
Master in Biological Physics
60 credits

Department of Physics
Faculty of mathematics and natural sciences

UNIVERSITY OF OSLO

Spring 2020

Computational Neuroscience for the Clinic :

Transcranial stimulation for Parkinson's Disease

Erin Beate Bjørkeli

Computational Neuroscience for the Clinic :

http://www.duo.uio.no/

Printed: Reprosentralen, University of Oslo

Abstract

In this theses we have studied the effect of electrical stimulation for treatment of Parkinson's disease by using both biopysically detailed models and larger scale models including different regions of the brain. We have found that the action potential firing in the soma can be stopped by electrical stimulation, which mainly effects the neurons. The stimulation has to be sufficiently strong in order to stop pathological firing, but too strong stimulation entraines the activity by starting action potentials in the cell's axons. The success of the stimulation depends on its amplitude and frequency, and also phase in the case of low frequency stimulation. The shape of the signal also ; square-pulses are good for starting action potentials in the axons while triangular signals are good for stopping firing in the cell. However, the Parkinson's disease seems to be due to pathologies in a larger circuit system, and resonance phenomena within this system could be the reason why stimulation close to the pathological frequency is not very successful for treating the disease. On the other side, the circuit nature makes it possible for stimulation to regions higher up in the brain, such as cortex, to affect the deeper regions. Cortical stimulation could therefor in theory not only reduce tremor in Parkinson's disease, but also treat the pathological activity underlying the condition.

Contents

List of Figures

List of Tables

CHAPTER 1

Introduction

Computational neuroscience has since its beginning in the 1950's made great contributions to the understanding of how our brains functions, from the level of single cells to larger networks, by the use of physics based models. In developing these models the focus has for the most part been on explaining "normal" neuron- or brain activity based on data from animal experiments. But not all brains are healthy. An obvious goal of the field should be to contribute to the understanding of pathological brain states in disease, and to how these can be treated, or possibly cured, in a safe and effective manner ([Mak+19]).

One of the most studied brain diseases is Parkinson's disease (PD). Parkinson is a neuro-degenerative disorder, where patients are suffering from motor disturbances like tremor, rigidity, and bradykinesia. These symptoms are believed to originate from a system deep within the brain called the Basal ganglia (BG) ([Bro+01], [Bro07]).

Basal ganglia has particular involvement in motor control and has been shown to be important in the initiation (or non-initiation/"holding") of actions ([Mir+17]), the so called "fight or flight (or freeze)" response. The BG consists of multiple neuron populations that are interconnected in a circuit like way, and the characteristic shaking of Parkinson patients seems to involve dysfunction within these circuits. This has be observed as beta frequency oscillations, with frequencies between 12 and 30Hz, in some of the populations. Lesions to some of these populations, mainly the subthalamic nucleus, can stop these oscillations. Interestingly, in many patients the same effect can be reached by deep brain stimulation targeting the same areas, that is, by application of electrical electrodes placed inside the brain.

Deep brain stimulation has for the most part been done using high frequency stimulation (100-130 Hz) ([Cag+19]). This is believed to work by making the activity more irregular in the targeted population, which in turn decouples the synchronicity that caused the beta oscillations ([Ros+14]). However, this method is fraught with "leaking" of current to other neighbouring brain regions, and might also interrupt the normal activity of the BG. This can cause side effects, for instance higher impulsiveness in the patient. This comes on top of the innate invasiveness of the electrode implantation, which first has to be inserted into the brain and then later maintained, and the treatment might not be desirable for all.

While the normal approach has been to record and treat the pathological oscillations within the BG, the same oscillations can also be found in the (motor) cortex. This have given rise to theories of "Parkinson circuits", where multiple

regions of the brain helps generate and are affected by the malfunctions. This opens up the possibility of treating PD by stimulation targeting other sites than the BG where they originate. Stimulation to thalamus, which is part of the proposed circuit, has been effective in reducing tremor ([Cag+19]). However, stimulating thalamus does not markedly improve other PD symptoms such as rigidity and bradykinesia ([Cag+19]). One possible explanation for this could be that the thalamus stimulation is only modulating the "output" of the malfunctioning system, but that the stimulation fails to affect the source. The stimulation might have to go deeper.

An alternative method to DBS is transcranial stimulation (TCS), where the electrodes are placed on top of the patients scalp and targeting the motor cortex. This eliminates any surgical procedures and it simplifies maintenance like charging batteries, which might make it a more appealing alternative to patients and doctors alike. However, TCS requires stronger stimulation than DBS, and carries a risk of damaging tissue such as the skin under the electrodes ([Ant+17]). Low frequency stimulation is typically used in TCS, and sometimes the frequency is set to mach the tremor frequency in patients ([Cag+16]). The effect of the treatment has been shown to dependent on the phase of the stimulation, as well as its frequency and amplitude. Thus more fine tuning is required in order to effectively treat the the tremors compared to the more used DBS.

This project will study the mechanism of brain stimulation, with particular weight on the types used to treat Parkinson's disease. This will include models for the basal ganglia, both on the single cell level and more abstract models meant to capture the larger network behaviours, and whether models like these are suited to study the circuit like behaviour that underlies shaking in PD. Further, it is interesting to see if the response of the models are similar to what we would expect to based on experiments, and whether they can be used to suggest alternative ways of treating the disease.

CHAPTER 2

Theory

2.1 Neurons and Membrane Potentials

The cell membrane is a lipid bilayer that separates the cytoplasm inside of the cell from the extracellular medium, the fluids outside of cells. Inside the cell lays all the organelles for creating energy and the building blocks for life. Ions, such as sodium and potassium, are kept in different concentrations inside and outside the cell. The cell membrane in nearly impermeable to the ions and prevents the ions from diffusing to balance out the concentrations, which sets up a potential across the membrane. Floating in the membrane are special proteins, so called ion-channels, which allows for ions to flow through. The channels are typically ion-specific, meaning they are much more permeable to a certain ion-species than to others. Some channels are "passive" and will always be open for the ions to pass through, others are "active" and will alternate between an open and a closed state. The state of the active channel is decided by outside factors; voltage-gated channels will open up when the membrane potential reaches a threshold value that is either sufficiently high or sufficiently low depending on the channel, whereas ligand-gated channels requires certain molecules (ligands) to bind to the gate in order to open (or close) and depends on the concentration of this molecule. This type of channels are responsible for the majority of current across the cell. As ion channels open and close they cause a spurt of currents. This changes the membrane potential, and if it passes a threshold value, an action potential (AP) is fired. The AP is characterized by a rapid depolarization of the membrane before it repolarizes, and possibly hyperpolarizes, and goes back to the resting potential. The transfer of the action potentials is what allows cells to communicate with each other. The cells contains a vast pool of ions, but for the activity to continue over time, the cell has to be "recharged" by restoring the concentrations on the inside and outside of the membrane. This is managed by ion-pumps that move the ions against their concentration gradient by expending energy. The most pump for maintaining the membrane potential in cells is sodium-potassium pump, which is illustrated in figure 2.1 along with sodium and potassium channels.

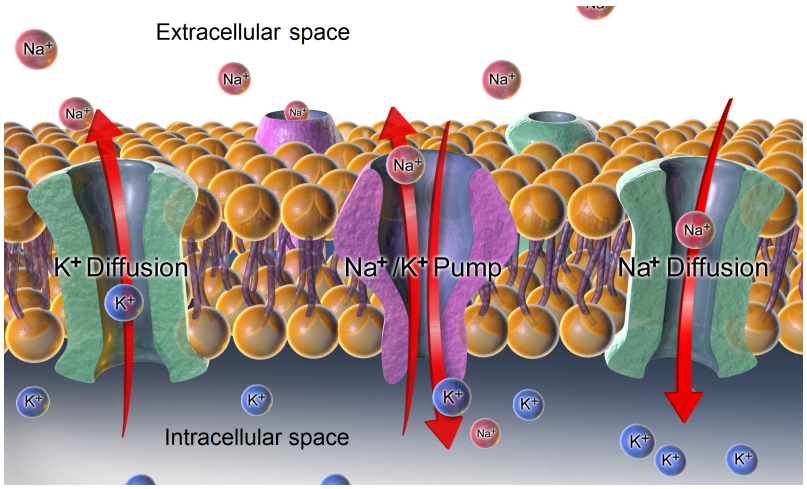

Figure 2.1: The cell membrane divides the intra- and extracellular fluids, and is nearly impermeable for ions. Different proteins allows for the ions to pass; ion channels (left and right in figure) lets the ions move in the direction of their concentration gradients and are typically ion-specific. Active ion-channels are required for neural firing. Ion-pumps (middle of figure) are able to move ions against their gradient by spending energy. This maintains the membrane potential, keeping the cell functional. The figure is borrowed from Blausen.com staff (2014). "Blausen gallery 2014". Wikiversity Journal of Medicine. DOI:10.15347/wjm/2014.010. ISSN 20018762.

Neurons are distinguished from other cells mainly by having axons and dendrites, which makes the neurons able to connect and communicate with each other. These are long narrow cables extending from the soma, the main body of the cell. The dendrites receives input from neighbouring cells and the axon pass on the electrical impulse to other connected cells. The site of connection is called a synapse. When an AP arrives at the end of an axon, a chemical synapses will release neurotransmitters (signal-molecules) at the presynaptic site which diffuse over to the post-synaptic cell. Electrical synapses are proteins bridging the gap between an axon and a dendrite that lets current pass directly. The connection can be excitatory, which makes it easier for the postsynaptic cell to fire an action potential, or inhibitory, lowering the membrane potential of the receiving neuron so that initiating action potentials require stronger inputs to reach the AP threshold.

2.2 Multi-compartment Modeling

With its long and thin extensions, the neurons membrane is not isopotential. For a model to faithfully capture the activity of a neuron, it has to be modeled as having multiple compartments.

In a multi-compartment model, the neuron is spilt into multiple cylindrical segments, and for each segment we can calculate the currents running through the membrane or to the neighbouring segments. This should fulfill Kirchof's law by the sum of the currents entering and leaving a compartment is zero. Each segment is assumed to be isopotential, so how many segments the model

should be divided into has to be evaluated based on the cells morphology. A trade off between accuracy and computational load has to be made.

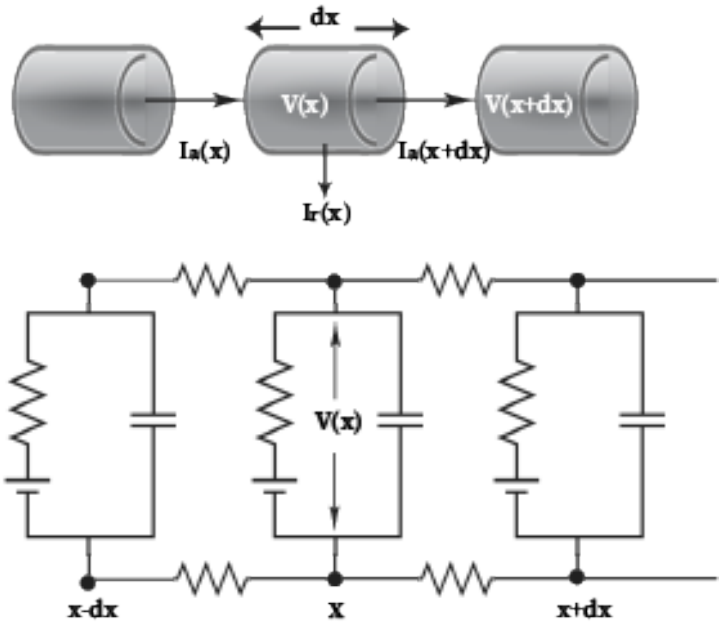

Figure 2.2: Multi-compartment modeling. The membrane potential (or change of) of compartment x of a neuron can be calculated by evaluating the currents entering and leaving the compartment radially I_r, as well as the currents passing between the compartments axially I_a.

For infinitesimally small compartments, the compartment modeling leads to the cable equation for describing the potential along the membrane:

$$C_m \frac{\partial V_m}{\partial t} = \frac{V_m - E_m}{R_m} + \frac{d}{4Ra} \frac{\partial^2 V_m}{\partial x^2} + I_s$$

On the left hand of the equation V_m is the membrane potential and C_m is the membrane capacitance. On the right hand, E_m the reversal (resting) potential, ie. the potential where the membrane is in equilibrium, R_m is the resistance over the membrane (radial), R_a is the axial resistance and I_s is any additional current, such as the current from conductances that are active during subthreshold potentials, or synaptic currents.

2.3 External Electrical Fields

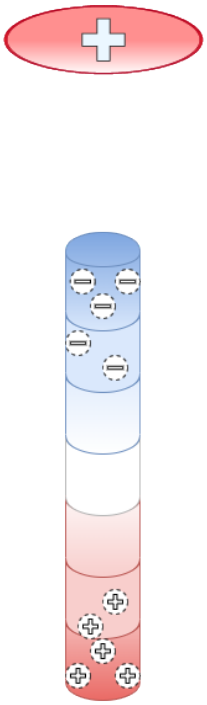

Figure 2.3: Polarization of the stick-neuron due to the electric field from a far-away electrode. The electric field causes the ions within the cell to move, causing them to cluster towards ends. This creates a polarization over the neuron, where the midpoint is neutral. More complex morphology, like branching in the neuron, will complicate where the ions are funneled.

When a cell is stimulated by electrodes placed far away, an electric potential is set up in the area surrounding the cell. The electric field effects the cell by displacing the ions within it, which changes the membrane potential along the cell. This is illustrated for a simplified stick-neuron in figure 2.3. Some parts of the cell will be depolarized by having more positive and/or fewer negative ions than in the resting state, and vice versa will other parts be hyperpolarized. For example, if the electric potential is aligned so that it is positive above the cell, the positively charged ions such as sodium will be forced towards the bottom of the cell. This will cause a build up of charge and a depolarization in this region (basal), while the top (apical) with the equal "lack" of positive charges will become hyperpolarized. The midpoint will be neutral if the neuron is approximated to be cylindrical; a more complex morphology complicates this. If the depolarization of a region that can fire APs is sufficient, a spike will be fired.

To evaluate the effect of the electric field on the cell membrane, the external field potential V_e is included in the cable equation ([GR16]). Ephaptic coupling

between neurons is one type of external electric fields, and the field from an electrode can be modeled in the same way:

$$C_m \frac{\partial V}{\partial t} = \frac{E_m - V_m}{R_m} + \frac{d}{4Ra}\frac{\partial^2 V_m}{\partial x^2} + \frac{d}{4Ra}\frac{\partial^2 V_e}{\partial x^2} + I_s$$

In order to decide the electric potential V_e outside the cell, we have to consider how currents are conducted from the electrode to the cell.

2.4 Volume Conduction and Non-isotropic Media

The electric potential V_e will fall proportionally with the distance moved away from its source (the electrode). The current I_e injected into a media will set up the electric field:

$$V_e(r) = \frac{I_e}{4\pi\sigma r}$$

where σ is the conductance of the media (assumed to be infinite and homogeneous) and r is the distance from the electrode.

If we instead consider that the conducing media is finite and surrounded by air which acts as an insulator, this becomes ([Nes+15]):

$$V_e(r) = \frac{I_e}{2\pi\sigma r}$$

The human head is not a homogeneous medium. Trans cranial current stimulation has to pass through the skull and ceberospinal fluid as well as the brain tissue, and these have different electrical conductivities than brain tissue. For modeling the passing of current through the head, the four-sphere volume conductor model can be used ([Næs+17]). The head is thought of as a sphere where the different constituents of the head (brain, cerebrospinal fluid, scalp and skull) are layers of the sphere. Each layer has a constant thickness throughout and a constant electrical conductivity within the layer. The sphere is surrounded by air. The Poisson equation

$$\nabla * \sigma(r)\nabla_e(r,t) = -c(r,t)$$

for this system can be solved numerically by finite element method, which gives the four-sphere model. Again, c is the current-source density, and Φ the electrical potential.

A different approach to conduction is to build a model based upon experimental data. Electrical lead fields can be constructed based EEG. Current is injected via the measuring electrodes and is solved for the potential throughout the head (by finite element modeling). The potential at the different points along the cell can then simply be found as the product of the field and current

$$V(r) = E_e(r) * I_e$$

where E_e is the electric lead field from the model. The New York Head model is an example of such an approach.

In this theses, the conductances in table 2.1 will be used.

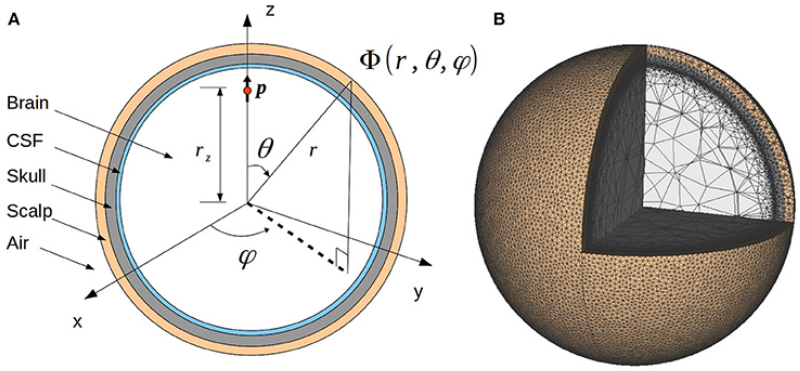

Figure 2.4: Illustration of the four-sphere model. The head is modeled as a sphere with multiple layers. The layers are different mediums in the brain, brain, CSF, skull and scalp surrounded by air, and have a thickness (measured as radius) and an electrical conductivitis. The current dipole moment p lays within the head. Reprinted from "Corrected Four-Sphere Head Model for EEG Signals," by S. Næss et al., 2017, Frontiers in Human Neuroscience, Volume 11

Media	Conductance σ [S/m]
Brain	0.3
CSF	1.5
skull	0.015
Scalp	0.3

Table 2.1: Conductances of the various medias of the brain.

2.5 Measuring Neuron Activity

The current entering a cell has to be balanced by a current exiting the cell in order for current concervation. From the viewpoint of the extracellular medium, current going out of the cell, will be seen as a current source, and similarly current flowing into the cell as a current sink. This means sodium ions (Na^+) moving into the cell would be a sink. This activity can be picked up by an electrode. Again we can use volume conduction theory to calculate the potential that would be measured by the electrode.

Measuring brain activity can be done with various methods. ECoG (electrocoticography) is done with an electrode placed on top of cortex. ECoG can be measured with the same electrodes used for deep brain stimulation, limiting the extent of operations. Another recording method is EEG (electroencephalogram), which is measured on top the patients scalp. With EEG the different conductive medias in the head has to be considered.

For both methods the signal that is measured is the contribution from many cells, typically thousands to tens of thousands, and it is not possible to single out the activity of a single cell ([12]). The same is true when we are trying to stimulate the cell, and spilling of current to nearby areas is a concern during brain stimulation.

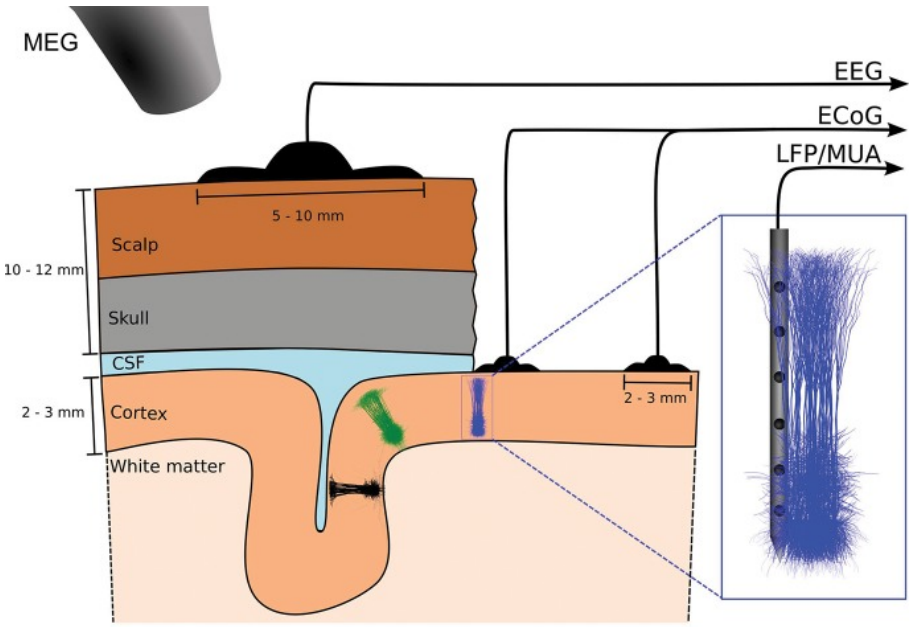

Figure 2.5: The electric and magnetic signals from neurons in the cortex can be measured at different levels. The signals intensity falls off with distance, and in modeling the different materials between the neuron and the recording electrode (e.g. scalp and skull) has to be taken into account. Figure borrowed from Hagen et. al [18]

Current Dipole Moment

When current enters a neuron, this should be balanced by a current exiting the neuron for charge conservation. As described before, this can be envisioned as a current source and a current sink. The two-compartment model in figure 2.6 shows the simplest model for this, where the dendrite is the current sink and the soma the current source. The extracellular potential generated by the neuron activity can be evaluated in terms of the different multipoles of the currents.

$$V_e = \frac{dipole}{r^2} + \frac{quadrapole}{r^3} + \frac{octupole}{r^4} + ...$$

However, when moving far away from the cell, the contribution of higher current pole moments will be vanishing. This means that if we measure from a sufficiently large distance, the potential can be modeled using only the current dipole moment.

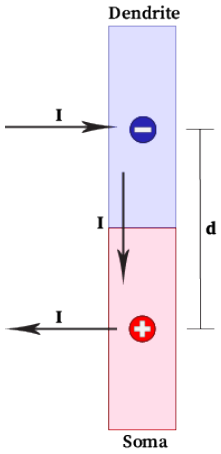

Figure 2.6: Current dipole moment in a two-compartement (soma and dendrite) cell. Current entering the cell in the dendrites looks like a current sink from the point of view of the extracellular space. This current is balanced by a current out of the cell in the soma, in order to maintain the potential. This makes a current source for in the extracellular space.

Measured far away from the cell, e.g. at the electrode site, the extracellular potential follows the formula:

$$V_e = \frac{\vec{p} * \vec{e}_r}{4\pi\sigma r^2}$$

where $\vec{e}_r$ is the unit vector in radial direction and $\vec{p}$ is the current dipole moment. For a two-compartment model, the dipole moment is given as:

$$\vec{p} = I_a d \vec{e}_p$$

$\vec{e}_p$ is the unit vector in the direction from negative to positive current, I_a is the axial current along the neuron, and d is the distance between the sink and the source. This form can be extended for a multi-compartment neuron with N-compartments:

$$\vec{p} = \sum_{n=1}^{N-1} I_a^n d_n \vec{e}_p$$

d_n is the length of each current I_a^n.

2.6 Effect of Cell Morphology

Real neurons are not long, straight cables; they are full of branches and bends, and the specific morphology will effect how the neurons respond to the external electric potential ([ALO16], [ARO18]). In part this is caused by the specific channels and their distribution along the axons and dendrites, but also how ions are spread between different compartments when the external potential changes. For example, the same amount of ions being pushed into a single axon will depolarize the membrane more here than the same amount being

spread between the branches in the dendritic-tree with its larger membrane area. Therefor, the polarization might be stronger in some locations, and this is important for where the voltage-gated channels activate. Axons again might respond different from dendrites. They typically have a larger and more unchanging radius than the dendrites. This will effect the axial conductivity of the neuron, as it is proportional to the radius of the cell/compartment:

$$\sigma_a = \frac{1}{R_a} = \frac{1}{R}\frac{A}{l}$$

Here R_a is (axial) resistivity inside the compartment and R the resistance, l the length of the compartment and A its cross-section. Another important difference is that the axons are able to fire action potentials, something the dendrites do not. Especially the h-type channels, which are activated by hyperpolarization of the membrane, seems to affect the response to the external stimulation [ALO16], [NRE18]). These are typically spread out on the apical dendrites, with increasing densities away from soma.

Frequency Response in Neurons

Neurons will often have a frequency dependent response to alternating stimulation (2.7). Non-uniform distribution of the different ion channels, and the dynamics of the channels themselves is one of the reasons ([Ant+17]). When an action potential fires, the sodium channels are opened first causing a depolarisation of the membrane and gives a transient current until their inactivation. The potassium channels opens later, but stays open for a longer time. If the frequency is too low, the potassium channels will start opening before the sodium channels are "fully" open, and the two currents will balance so that the maximum possible potential, in relation to the specific stimulus, is not reached.

If the stimulation frequency is too high on the other hand, the sodium channels will not have time to react to the change in voltage. The change of conductance is dependent on the change in voltage ($\frac{\delta g}{\delta t} \propto \Delta V$) ([Ste14]). The time resolution of the gates are about 1 ms, and the intrinsic low pass filtering in the membrane means that frequencies above 1 kHz will typically not register ([Gro+17]).

It has also been suggested that some amount of filtering can happen outside of the neurons, when the stimulation (or electrical potential from the cell) is passing between different medias in the head ([BKD18]). However, as this is a disputed topic we will assume the conductivity to be independent of frequency.

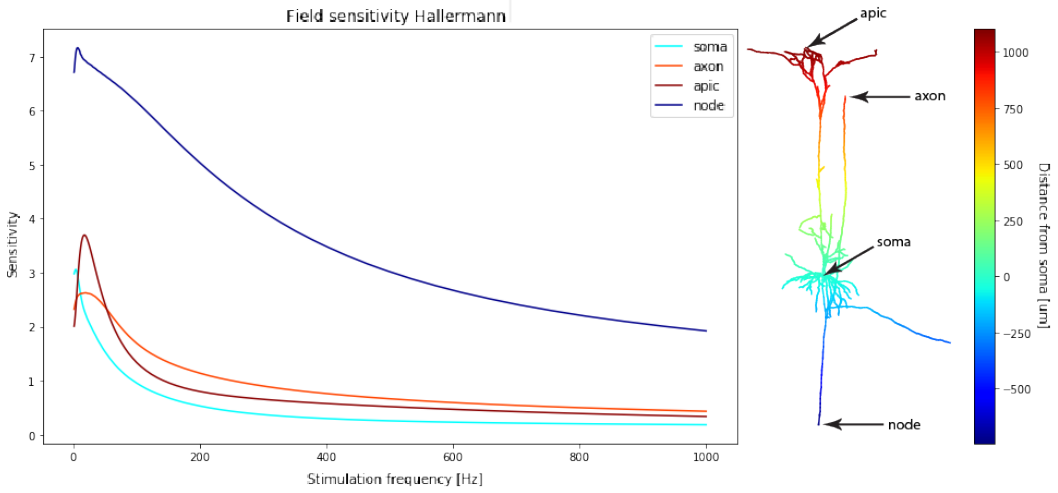

Figure 2.7: Frequency response in Hallermann cell. The response is measured by the amplitude of the membrane potential during subthreshold oscillations, and is evaluated at the soma, the upwards axon (axon), the top of the apical dendrites (apic) and the lowest axon (node). Resonance is seen for lower frequencies, while the membrane polarization is much smaller for higher frequencies.

2.7 The Basal Ganglia and Parkinson's Disease

The Basal Ganglia (BG) is a structure located in the deep of the brain involved in motor control. BG is believed to control the initiation or holding of action, causing a "fight or flight" or "freeze" response. The basal ganglia consists of multiple neuronal populations that are mutually connected.

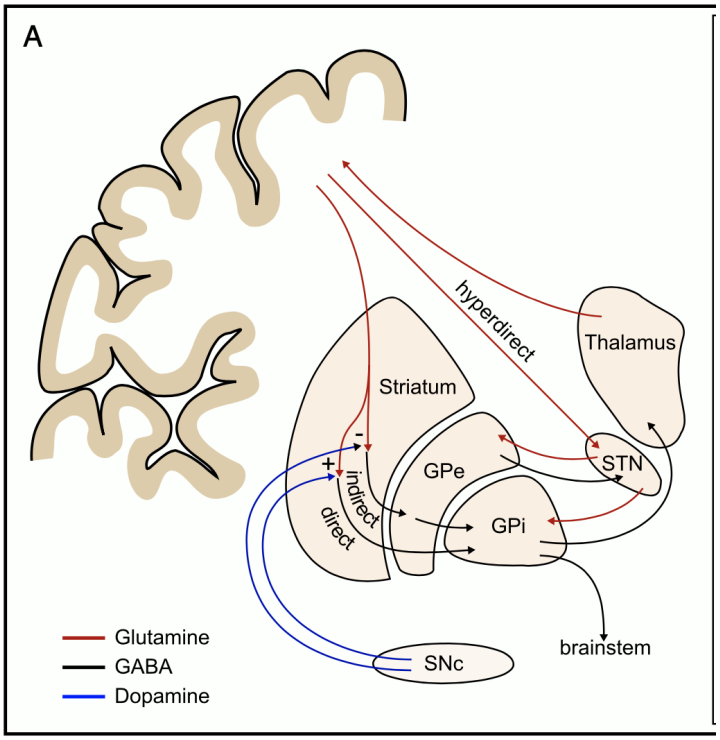

Figure 2.8: Illustration of the basal ganglia. Reprinted from "Oscillations and the basal ganglia: Motor control and beyond," by J. S. Brittain and P. Brown, 2013, NeuroImage, Volume 85, part 2, p. 637-647. Copyright [2013] by Elsevier Inc.

On top is the striatum. It receives input from the cortex and relays signals down to the basal ganglia via various pathways. The striatum consists of mainly two sub-populations of medium spiny neurons (MSN), D1-MSN and D2-MSN, which differs in their dopamine receptors. Typically, the D1 population has a higher activity than D2, but in the case of Parkinson's disease this is observed to switch ([Bah+17], [BB13]). As the populations sends signals through different pathways to the output nucleus (GPi) of the BG, this is hypothesized to be a significant part of PD.

The change in the activity of D1 and D2 are thought to be caused by changes in the pars compacta part of the substantia nigra (SNc). The SNc seems to regulate the activity of striatum, and contribute to fine motor skills. PD is characterized by a death of neurons in this population. This causes dopamine depletion in striatum, and medication used for PD tries to replace the dopamine.

The D2-MSN is connected with the globus pallidus externus (GPe). GPe has two sub-populations, TA (arkypallidal) and TI (prototypical) neurons. GPe-TI mainly signals downstream in the basal ganglia to the GPi and STN and makes up about 75% of the population, whereas GPi-TA signals back to the striatum in a feedback loop. In our model we have chosen to only include the GPe-TI population to simplify the dynamics, and from here on GPe will refer to this population only. The path down BG going through GPe is called the indirect pathway.

Interconnected with the GPe is the subthalamic nucleus (STN). The STN is a population of excitatory neurons, and receive input from the cortex that is relayed to the GPi; this is called as the hyperdirect pathway. The STN has long been known to play a part in the tremoring in PD; the beta oscillation can be measured here, and both lesions and electric stimulation to the STN have been effective for treating PD.

Globus pallidus internus (GPi) functions as the output nucleus of the BG. It receives input from STN, GPe and D1 through the hyperdirect, indirect and direct pathways respectively. In PD the balance between activity from the different pathways is disrupted; the indirect pathway becomes stronger than the direct one when there is reduced dopamine in the striatum ([Bah+17]). Reduced projection through the hyperdirect pathway, as in PD, seems to cause symptoms with lack of movement like bradykinesia. The GPi further inhibits parts of the thalamus. Thalamus is then connected to the cortex, and thus closes the cortico-thalamo-basal ganglia circuit.

2.8 How to treat Parkinson's Disease

Parkinson's disease has typically been treated with high frequency stimulation (100-130Hz) delivered to deeper brain regions, typically to the STN ([Cag+19]). This is believed to work by introducing "noise" to the activity in these regions by inducing more frequent and regular spiking, which in turns "breaks" the firing synchronicity that are causing beta oscillations in the region. Short time depression of the synapses going from STN to connected regions might also be part of the mechanism for desynchronization ([Ros+14]). The effect of the stimulation will be dependent on the amplitude and frequency of the stimulation, but not on its phase. High frequency stimulation has also been tested on the thalamus. This seems to be able to reduce the tremor in patients, but not in helping with rigidity and other dyskinesias ([Cag+19]).

There are also side-effects to the high frequency stimulation. One is that it makes the patients more impulsive, which is similar to what is seen when PD-patients are treated with dopamine ([Cag+19], [BAK15]). This could be due to disruptions of the normal activity in the basal ganglia. Delivering relatively large amount of current could also lead to current affecting the regions surrounding the target.

Stimulating at much lower frequencies has been proposed as an alternative. The hope is that this would more directly targeting the pathological oscillations and not disrupt the normal activity in the basal ganglia, and that this could reduce side effects. Other benefits could be it requiring less energy which would extend the battery life in electrodes. In experiments this treatment has been found to require more tuning, since it is both frequency and phase dependent, besides having the strength of stimulation be fitted to the patient ([Cag+14], [Bri+13], [Hol+18], [Cag+19]). This suggest it is functioning by different mechanisms than high frequency-stimulation, possibly by stopping action potentials by altering the threshold for firing.

As the beta oscillations can be measured in the cortex, this has also been suggested as a possible site for treatment. Trans-cranial stimulation (TCS) has been tested, and can reduce shaking in patients ([Bri+13], [Hol+18]). This has only been found to work with lower frequencies. TCS is analogous to EEG

in that the electrode is placed on top of the scalp. This is less invasive than classical treatment of PD, and makes maintenance easier.

2.9 Parkinson circuits

The beta oscillations seen in the BG are also measurable in cortex and thalamus, and since the BG receives input from the cortex, this neatly closes a circuit. The oscillations could stem from multiple mechanisms within this. One theory is that the oscillations comes from the changes just within the STN-GPe circuit ([Wes+18]). Another possibility is that it is created by a larger circuit; degradation of the substantia nigra is a trait of PD, and it has been shown that these populations can regulate initiation of movement. This is called the "dimmer-switch" model. An even longer loop could be possible where the oscillations is driven by the feedback back to cortex in the cortico-thalamo-BG circuit. The three can be seen in figure 2.9.

The different models will respond different to treatment. If the oscillations are a phenomena contained to the STN-GPe circuit, this might be the only place they can be stopped. The other models might not be as contained. If the input to BG is part of driving the oscillation, they might be corrigible higher up in the brain.

Stimulation to the thalamus can reduce the tremor, but does not treat other PD symptoms [Cag+19]). Some experiments with trans-cranial stimulation targeting the cortex have been more promising ([Cag+14]), but whether cortical stimulation actually stops the pathological oscillations or merely functions as a form of output modulation is not clear, and the fact that only low frequencies ("tremor frequencies") have been successful suggest there might be other frequencies in the cortex contributing to the shaking in patients.

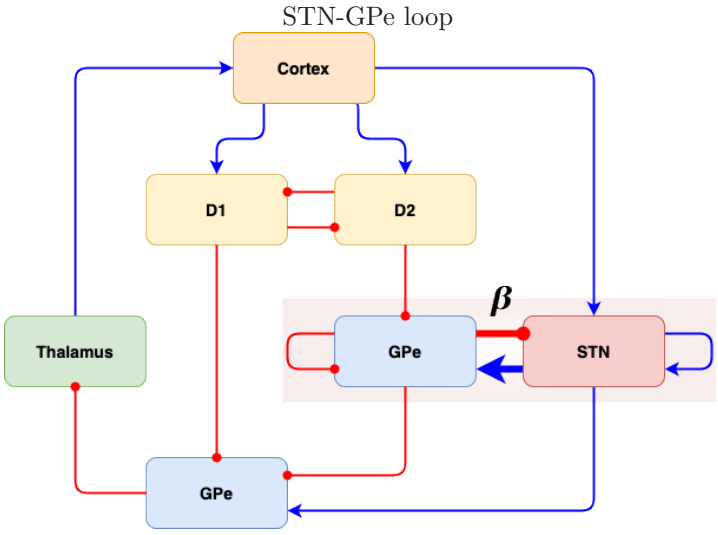

Figure 2.9

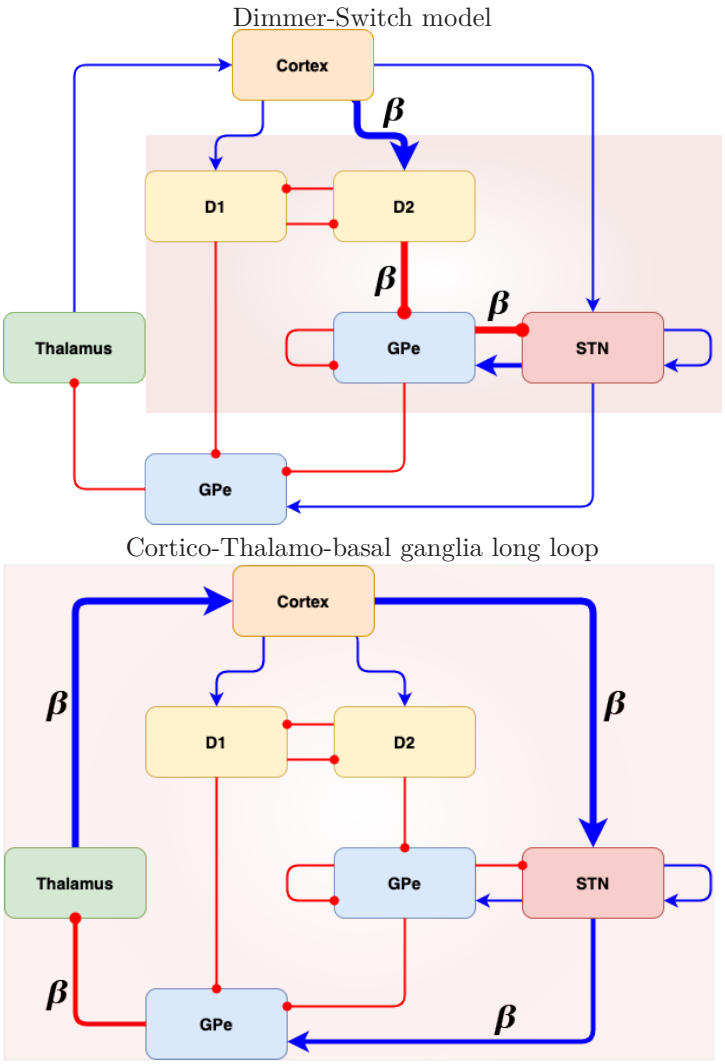

Figure 2.9: Three possible circuit models for the generation of beta-oscillations for Parkinson's disease. UPPER: The oscillations are created by alterations in the connections between STN and GPe. MIDDLE: The "dimmer-switch" model, which suggests that the oscillations stated between STN-GPe are controlled by the cahnges in activity in straiatum. LOWER: The beta-oscillation are created by the feedback between cortex and basal ganglia.

CHAPTER 3

Methods

The simulation of single cells were done in python using the LFPy package.

3.1 Setting up the Simulation

Synaptic Input and Electric Field

To create a parkinsonian activity in the neuron, synaptic input of 20 Hz was injected to the soma. The input was created by setting an array with the spiketimes with a regular period, before random jitter was added to the stimulation to slightly alter the spiketimes. This made it so that occasionally one period would pass without a spike firing, as is seen in figure 4.5 at 200 ms. The synapse was created with the $LFPy.Synapse$ class and the spiketimes set with the function set_spike_times.

The function $LFPy.insert_vext$ was used to insert the external electric potential, which had been calculated for the midpoint of each compartment of the cell model.

Different Volume Conductors

To model brain stimulation and measurement, we used different types of volume conductors. The most basic is the infinite, homogeneous media. A brain-volume surrounded by air was assumed. This was modeled as described under section 2.4.

The second approach is using the Four-spheres-volume-conduction model, also mentioned under section 2.4, which is included in the LFPy-package and can be set up with the $LFPy.FourSphereVolumeConductor$ function. For this, the values in table 2.1 were used.

Another way to go is using head models built form from experimental data. The New York Head model is a electric lead-field model based on MRI-scans of different heads ([Dmo+17]). It has a resolution of $0.5mm$, which is impressive for EEG measurement, but not so impressive when looking at the scale of a single neuron. To make the field useful, we interpolated values from neighbouring points in the NY-head data, by assuming linearity in the media.

To use the data, the electrode of which to measure (or stimulate) from has to be chosen. The electrode nr. 19 seems to be placed close to the motor cortex, and was used as the standard choice in the model. An electrode could also be picked based on coordinates.

The potential field at the cell is then calculated from the lead field as:

$$V = E * I(r)$$

Where E has been calculated in the NY Head model, and $I(r)$ is the current strength at distance r.

The values from this data seemed a bit of; when compared to the result from other head models it was approximately one order of magnitude larger. We adjusted for this by dividing the results by 10.

The lead field was downloaded from *parralab.org/nyhead/*.

Modeling EEG

The EEG is calculated by recording the dipolar moment during the simulation, which can be done by LFPy by specifying $rec_current_dipole_moment = True$ in the $LFPy.simulate$ function, and then combined with the conduction model that is used (homogeneous, 4-spheres, NY-head). This is repeated and summed up to simulate the recording of many neighbouring neurons under the electrode. A low pass filter is applied, as is done for actual EEG measurements.

Cell Models

In our simulations we mostly used the Hallermann model neuron ([Hal+12]). This is a layer 5 cortical pyramidal neuron. An axon extends upwards, parallel with the apical dendritic tree. This makes the model good for studying what effect the direction of axons might play in response to stimulation from an external electric field.

Closed-loop Stimulation

A closed-loop approach has many benefits compared to continuous stimulation; it reduces the power use and thus increases the battery life. It is also able to adjust to changes in the activity, like "slipping" which causes a phase shift. Slipping could possibly occur if the synaptic input was changed.

The closed-loop stimulation is done by periodically recording the brain signal (eg. the EEG), and resetting the stimulation features based on this. As a "proof of concept", we started by recording and averaging the LFP from multiple simulations with no stimulation. The peak beta-frequency was picked from the FFT spectra. The phase was found from the cross-correlation of the measured signal and a sine wave of 20 Hz using *scipy.signal.correlate*. The current dipole moment was used as a stand in for the EEG to reduce computation. The frequency was determined using the fourier transform, with $Numpy$ and its fft package. The stimulation was then applied with using the phase and the closest integer to the frequency.

We used a preset amplitude for the stimulation, but an amplitude could be found for example by checking the reduction of beta-power in the FFT, and adjust until this was maximally reduced.

Irregular Firing and Adaptive Stimulation

To do simulations with adaptive brain stimulation, we started by altering the synaptic input to the cell so that after some periods the phase was slightly

shifted. The stimulation was then made to adapt to this by every period checking the phase of the spiking (by cross-correlation with a $20Hz$ sine wave) for the past period. The stimulation phase is adjusted accordingly.

3.2 Setting up a Population Model

To study the effect of brain stimulation on the larger circuits involved in PD, we set up a Wilson-Cowan model similar to the approach of Yousif et al. ([You+17]) for essential tremor. The model is based on the "dimmer-switch" theory of PD, which assumes that the tremors of patients comes from interactions within and between two circuits: the basal ganglia and the thalamo-cortical circuit. The beta-oscillations are assumed to be created in the basal ganglia, and are caused by the altering of inputs from the degenerated striatum. The pathological signal then passes back to cortex via the thalamus, where they cause the characteristic tremors.

The model consists of one first-order coupled differential equation per region, in total 7 equations.

$$\tau_{Cx}\frac{dE_{Cx}}{dt} = -E_{Cx}(t) + (k_e - E_{Cx}(t)) * Z_e(w_{15}E_{Thm}(t) + Ext_1)$$

$$\tau_{D1}\frac{dI_{D1}}{dt} = -I_{D1}(t) + (k_i - I_{D1}) * Z_i(w_1E_{Cx}(t) - w_4I_{D2}(t))$$

$$\tau_{D2}\frac{dI_{D2}}{dt} = -I_{D2}(t) + (k_i - I_{D2}) * Z_i(w_2E_{Cx}(t) - w_5I_{D1}(t))$$

$$\tau_{STN}\frac{dE_{STN}}{dt} = -E_{STN}(t)+(k_e-E_{STN}(t))*Z_e(w_3E_{Cx}(t)-w_7I_{GPe}(t)+w_9E_{STN}(t))$$

$$\tau_{GPe}\frac{dI_{GPe}}{dt} = -I_{GPe}(t)+(k_i-I_{GPe})*Z_i(-w_6I_{D2}(t)+w_8E_{STN}(t)-w_{10}I_{GPe}(t))$$

$$\tau_{GPi}\frac{dI_{GPi}}{dt} = -I_{GPi}(t)+(k_i-I_{GPi})*Z_i(-w_{11}I_{D1}(t)-w_{12}I_{GPe}(t)+w_{13}E_{STN}(t))$$

$$\tau_{Thm}\frac{dE_{Thm}}{dt} = -E_{Thm}(t) + (k_e - E_{Thm}(t)) * Z_e(-w_{14}I_{GPi}(t) + Ext_2)$$

Where e denotes an excitatory population and i an inhibitory one. τ_p is the time constant, which we will assume is the same for all populations. Both the cortex and thalamus receives some external input from brain regions not included in the model, creating a baseline activity in the compartments that will drive the activity of the circuit. For thalamus, this could be input coming from the cerebellum.

Z is the sigmoid activation function. It describes what amount of "neurons" in the population that would fire (reach above a threshold) given the same excitation x when the neurons have a distribution either of thresholds or of number of synaptic connections. The most left hand term of the function shifts

the activation functions so that in the resting state with no input, $x = 0$, the populations are inactive or in a "resting state".

$$Z_p(x) = \frac{1}{1 + exp(-a_p(x - \theta_p))} - \frac{1}{1 + exp(a_p\theta_p)}$$

The function has been fitted by the criteria described by Wilson and Cowan ([WC72]), so as to have a system with an unstable steady state. The criteria are fulfilled, along with some restrictions of our own, with the parameters $a_e = 9.0$, $\theta_e = 4.0$, $a_i = 1.0$ and $\theta_i = 3.7$. This causes looping in the cortex-D2-GPe-STN sub-circuit when the activity in D2 is increased, as is the case in PD.

The system of equations were solved by forward-euler method in a custom-written python script.

The above system of differential equations can be written in matrix form:

$$\tau\dot{X} = -X + Z(A * X + B + S)$$

$$X = \begin{pmatrix} E_{Cx} & I_{D1} & I_{D2} & I_{GPe} & E_{STN} & I_{GPi} & E_{Thm} \end{pmatrix}^T$$

with the derivatives

$$\dot{X} = \begin{pmatrix} E_{Cx}dt & I_{D1}dt & I_{D2}dt & I_{GPe}dt & E_{STN}dt & I_{GPi}dt & E_{Thm}dt \end{pmatrix}^T$$

the external input

$$B = \begin{pmatrix} Ext_1 & 0 & 0 & 0 & 0 & 0 & Ext_2 \end{pmatrix}^T$$

and the coupling matrix

$$A = \begin{pmatrix} 0 & 0 & 0 & 0 & 0 & 0 & w_{15} \\ w_1 & 0 & w_4 & 0 & 0 & 0 & 0 \\ w_2 & w_5 & 0 & 0 & 0 & 0 & 0 \\ 0 & 0 & w_6 & w_{10} & w_8 & 0 & 0 \\ w_3 & 0 & 0 & w_7 & w_9 & 0 & 0 \\ 0 & w_{11} & 0 & w_{12} & w_{13} & 0 & 0 \\ 0 & 0 & 0 & 0 & 0 & w_{14} & 0 \end{pmatrix}$$

S is the vector of stimulation applied to different populations. In the untreated case $S = 0$.

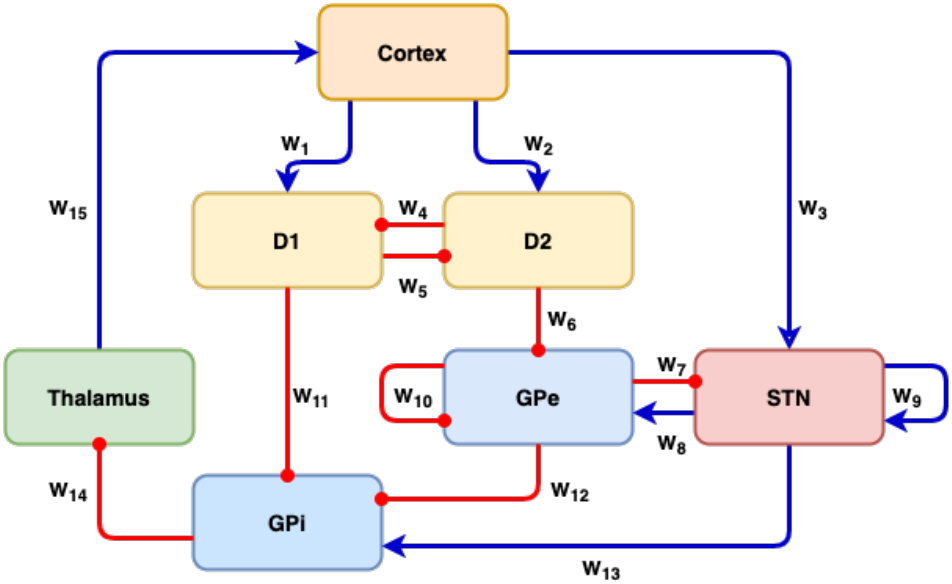

Figure 3.1: Sketch of a cortico-thalmo-basal ganglia circuit. Blue connections denote excitatory synaptic connections, while red are inhibitory.

The Jupyter Notebooks with the model can be found at: https://github.com/ebjorkeli/Parkinson-model

Fitting the Weights

In order to fit the weights between the populations, the model is set to fulfill the following conditions:

Healthy	Parkinson
Low activity in D2	Increased activity in D2
Low activity in D1	Decreased activity in D1
No oscillations (or high frequency)	Beta oscillations (20 Hz)

Table 3.1: Differences in the healthy and the parkinsonian state used as conditions for fitting the Wilson-Cowan model.

Furthermore, the beta oscillations should at least be visible in STN and cortex, where they have been recorded in experiments. Observations at other sites are more disputed, and is therefor not a requirement for the model. The oscillations should stem from the STN-GPe loop, although a larger circuit could be involved in starting the oscillations (ie. the oscillations can not be generated between the populations in the striatum or any other of the smaller circuits). If it is possible to stop the oscillations by addition of external stimulation to populations, most importantly STN as is done in DBS, the model could be useful in studying circuit behaviour of tremors.

We began the fitting in a reduced system that included only the compartments involved with the oscillations: the Subthalamic nucleus and the external

Globus Pallidus, with excitatory input from cortex to drive activity and inhibitory input from D2 in the Striatum. Increased activity in D2 is assumed to be the main cause of oscillations. After the system reaches a steady state, we assume the activity in cortex and D2 to be near constant, and this allowed to study the isoclines for just the two populations STN and GPe. while varying the weights in both directions between STN and GPe and keeping the other weights constant. This was done for a lower and a higher value for the weight between cortex and D2, representing the non-parkinsonian and parkinsonian states. We are interested in areas where the fist is stable and the latter is not.

The fitting and the model is described in more detail in appendix A.

Connection			Weigth	
From	To	w	Healthy	Parkinson
Cortex	D1	w_1	8.0	
Cortex	D2	w_2	7.0 to 13.0	4.0
Cortex	STN	w_3	8.5	
D1	D2	w_4	1.0	
D2	D1	w_5	6.0	
D2	GPe	w_6	5.0	
STN	GPe	w_7	20.0	
GPe	STN	w_8	15.0	
STN	STN	w_9	2.6 or 0.0	
GPe	GPe	w_{10}	4.5	
D1	GPi	w_{11}	7.0	
GPe	GPi	w_{12}	1.5	
STN	GPi	w_{13}	20.0	
GPi	Thalamus	w_{14}	5.0	
Thalamus	Cortex	w_{15}	5.0	

External input		Value	
To	Name	Healthy	Parkinson
Cortex	Ext_1	4.1	
Thalamus	Ext_2	3.9	

Time constant		Value (ms)	
Population	τ	Healthy	Parkinson
Excitatory	τ_e	13.0	
Inhibitory	τ_i	13.0	

Table 3.2: Parameters of the Wilson-Cowan model of Parkinson circuits (Basal Ganglia and thalamo-cortical network). The weights between populations, external inputs and time constants are listed here.

Adaptive brain stimulation was done by finding the phase of the activity after a set period, and shift then signal in order to avoid entrapping of the activity.

Stimulation and Linearization

To study the effect of the stimulation, we evaluate the Jacobi matrix and eigenvalues for the system. In the ideal case, the stimulation should bring the system back to the healthy state, ie. the eigenvalues should be the same as for a healthy non-oscillating system.

In order to analyze the system, it needs to be linearized. We do this with an Taylor expansion, which we can then evaluate at a given state x_s.

$$f(x) \approx f(x_s) + \frac{df}{dx}(x - x_s) + \frac{1}{2!}\frac{d^2 f}{dx^2}(x - x_s)^2 + ...$$

In the Wilson-Cowan model we are always dealing with values between 0 and 0.5 (and sometimes negative values) for the population activity, so we can disregard the higher orders.

The derivative of the sigmoid function:

$$\frac{d}{dx}Z_p(x) = \frac{d}{dx}(\frac{1}{1 + exp(-a_p(x - \theta_p))} - \frac{1}{1 + exp(a_p\theta_p)}) = \frac{a_p exp(-a_p(x - \theta_p))}{(1 + exp(-a_p(x - \theta_p)))^2} = Q(x)$$

For a system with one excitatory and one inhibitory population on the forms:

$$\frac{dE}{dt} = F(E, I) = -\frac{E}{\tau} + \frac{k - E}{\tau}Z(\alpha_1 E + \beta_1 I)$$
$$\frac{dI}{dt} = G(E, I) = -\frac{I}{\tau} + \frac{k - I}{\tau}Z(\alpha_2 I + \beta_2 E)$$

the linearization can be written as:

$$\frac{d}{dt}\begin{pmatrix} E \\ I \end{pmatrix} = \begin{pmatrix} F(E, I) \\ G(E, I) \end{pmatrix} \approx \begin{pmatrix} F(E_s, I_s) \\ G(E_s, I_s) \end{pmatrix} + J(E_s, I_s) * \begin{pmatrix} E - E_s \\ I - I_s \end{pmatrix}$$

where (E_s, I_s) is an equilibrium point and J is the Jacobi matrix of the system

$$J(E, I) = \begin{pmatrix} F_E(E, I) & F_I(E, I) \\ G_E(E, I) & G_I(E, I) \end{pmatrix} = \begin{pmatrix} -Z(s_E) + \alpha_1(k - x) * Q(s_E) & \beta_1(k - E) * Q(s_E) \\ \beta_2(k - I) * Q(s_I) & -Z(s_I) + \alpha_2(k - I) * Q(s_I) \end{pmatrix}$$

To simplify our notation, s_x will refer to the stimuli population x receives from other population, itself and external sources.

The Jacobian for the basal ganglia model above will look like:

$$J(X) = \begin{pmatrix} a_1 & 0 & 0 & 0 & 0 & 0 & a_7 \\ b_1 & b_2 & b_3 & 0 & 0 & 0 & 0 \\ c_1 & c_2 & c_3 & 0 & 0 & 0 & 0 \\ 0 & 0 & d_3 & d_4 & d_5 & 0 & 0 \\ e_1 & 0 & 0 & e_4 & e_5 & 0 & 0 \\ 0 & f_2 & 0 & f_4 & f_5 & f_6 & 0 \\ 0 & 0 & 0 & 0 & 0 & g_6 & g_7 \end{pmatrix}$$

$$a_1 = -1 - Z(s_{Cx})$$
$$a_7 = w_{15}(k_e - E_{Cx}) * Q(s_{Cx})$$

$$b_1 = w_1(k_i - I_{D1}) * Q_(sD1)$$

$$b_2 = -1 - Z(s_{D1})$$

$$b_3 = w4(k_i - I_{D1}) * Q(s_{D1})$$

$$c_1 = w_2(k_i - I_{D2}) * Q_(sD2)$$

$$c_2 = w_5(k_i - I_{D2}) * Q_(sD2)$$

$$c_3 = -1 - Z(s_{D2})$$

$$d_3 = w_6(k_i - I_{GPe}) * Q_(sGPe)$$

$$d_4 = -1 - Z(s_{GPe}) + w_{10}(I_{GPe} - k_i) * Q(s_{GPe})$$

$$d_5 = w_{10}(k_i - I_{GPe}) * Q_(sD1)$$

$$e_1 = w_3(k_e - E_{STN}) * Q_(sSTN)$$

$$e_4 = w_7(k_e - E_{STN}) * Q_(sSTN)$$

$$e_5 = -1 - Z(s_{STN}) + w_9(k_e - E_{STN}) * Q(s_{STN})$$

$$f_2 = w_{11}(k_i - I_{GPi}) * Q_(sGPi)$$

$$f_4 = w_{12}(k_i - I_{GPi}) * Q_(sGPi)$$

$$f_5 = w_{13}(k_i - I_{GPi}) * Q_(sGPi)$$

$$f_6 = -1 - Z(s_{GPi})$$

$$g_6 = w_{14}(k_e - E_{Thm}) * Q_(sThm)$$

$$g_7 = -1 - Z(s_{Thm})$$

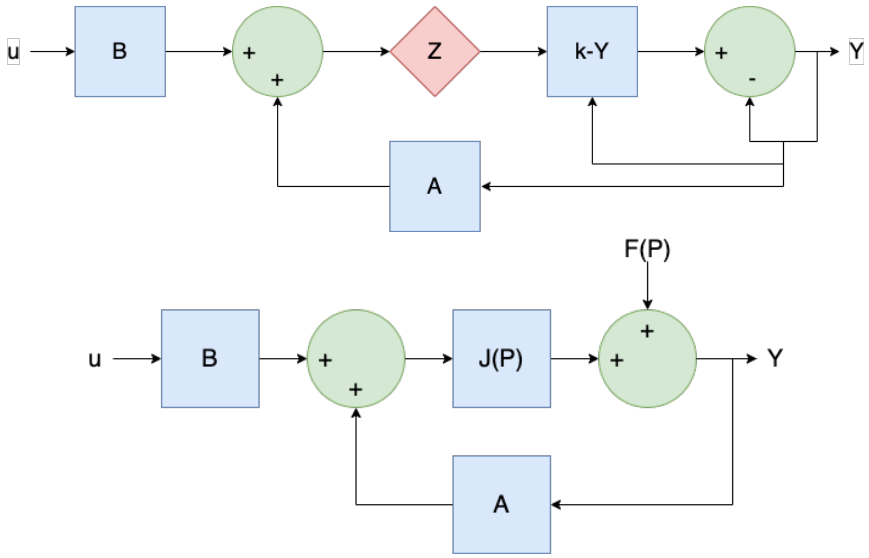

Figure 3.2: Block diagram of the model. On top is the nonlinear model with the sigmoid function Z. At the bottom is the linearized model, where the function F, the original function, has become a constant addition evaluated at the equilibrium point P.

CHAPTER 4

Results

We start with the results from simulations on the single-cell-level. The assumed goal here is to disrupt the regular firing in a cell with the external electric field set up by an electrode, and that this could reduce the beta oscillations in PD.

4.1 To Kill an Action Potential

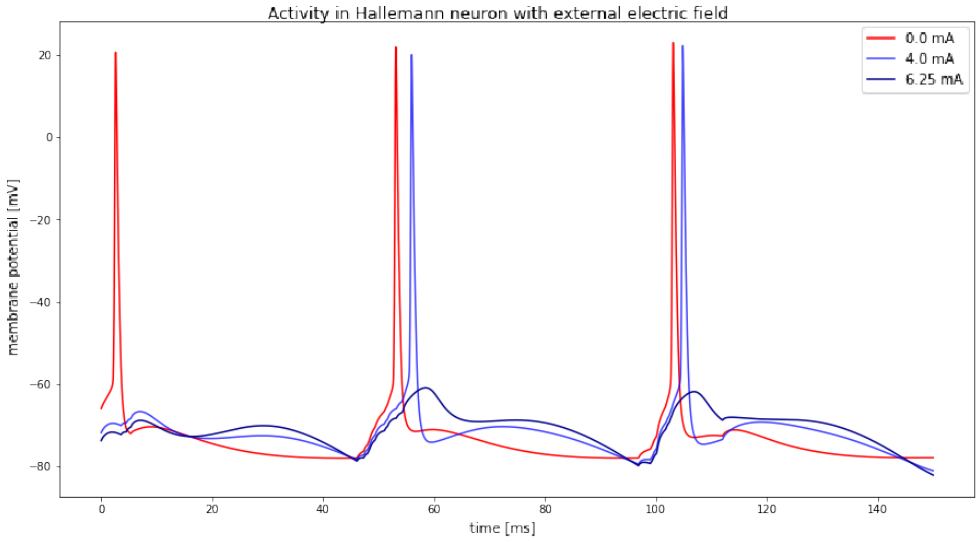

Figure 4.1: Spiking in Hallermann neuron is reduced with applied external electric potential. The neuron is initially firing at 20 Hz. When the potential is set by 4.0 mA current from the electrode, the first spike is stopped and the following two are delayed. When the current is turned to 6.5 mA all three spikes are prevented. Both the stimulation and the synaptic input was set to 20 Hz, and the strength of the synaptic connection to 7 nS.

The main activity of interest in neurons is what is called action potentials. During an action potential, the membrane potential sharply rises from its resting value, before rapidly going back to the normal resting value. Sodium and potassium are the main drivers of this process, but other ion-species

contributes to the shape of the action potential, and we say that its shape is characteristic (which channels are present can be deduced from the shape, however this is not a one-to-one problem).

The action potential starts by sodium flowing into the cell, which raises the membrane potential. If it reaches a threshold value, more sodium channels will open (voltage-gated) and a large amount of positive ions flow across the membrane, leading to a great depolarization. The sodium channels also have a closing mechanism, an inactivation variable, which kicks in after some time. At some point, the threshold voltage for potassium channels is reached, which leads to a repolarization of the membrane. Often a hyperpolarization, with a lower membrane potential than the resting value, will be reached before it goes back to the resting state ([Ste14]).

When we set synaptic input to our cells in the simulation, they generate action potentials firing at 20 Hz in the soma. It is not obvious that the AP generation in soma could be stopped by the electrical stimulation, which mainly affects the axons ([NB98]). Our simulations shows that is possible.

An alternating electrode current will cause the membrane potential to rise and fall proportionally to the strength of the electric potential the electrode, which moves the ions in the extracellular space. If this signal is aligned so that the most hyperpolarized state comes right before an expected action potential at the AP initiation site, it can result in the depolarisation not reaching the threshold for AP firing, and the AP is stopped. Experiments have shown that there is a phase dependency in low-frequency stimulation for PD ([Cag+14], [Bri+13], [Hol+18]), which would correspond well with a mechanism like this when the neural firing is regular.

4.2 Mechanism of Stopping Beta Oscillations

Low frequency stimulation works by altering the membrane potential, (OG?). This will alter with the electric potential over the cell. If the electric stimulation is adjusted properly to the neural activity, the cell will require a stronger synaptic input current in order to reach the threshold for firing. The strength of the electric field can then be set to quiet (mostly) all the action potentials.

Stimulating the Hallemann cell with high frequency stimulation (130 Hz, figure 4.2) sets of rapid firing of APs generated in the axons which then propagates towards the soma (antidromic firing). The axonal APs do not always propagate successfully to the soma. This can be seen in the bottom row of figure 4.2, where the activity is higher in the two axonal sites fires more frequently than the soma. At the end of the dendrites, this activity is barely noticeable, and no spikes can be seen as can be expected, since dendrites do not have the capability to propagate APs. Each firing of an AP in the cell affects the probability of a new AP for a short time, for example by the cell being in a depolarized or hyperpolarized state. The high frequency activity can therefor interrupt the regular firing in the cell. The phase of the signal plays no role in its effect.

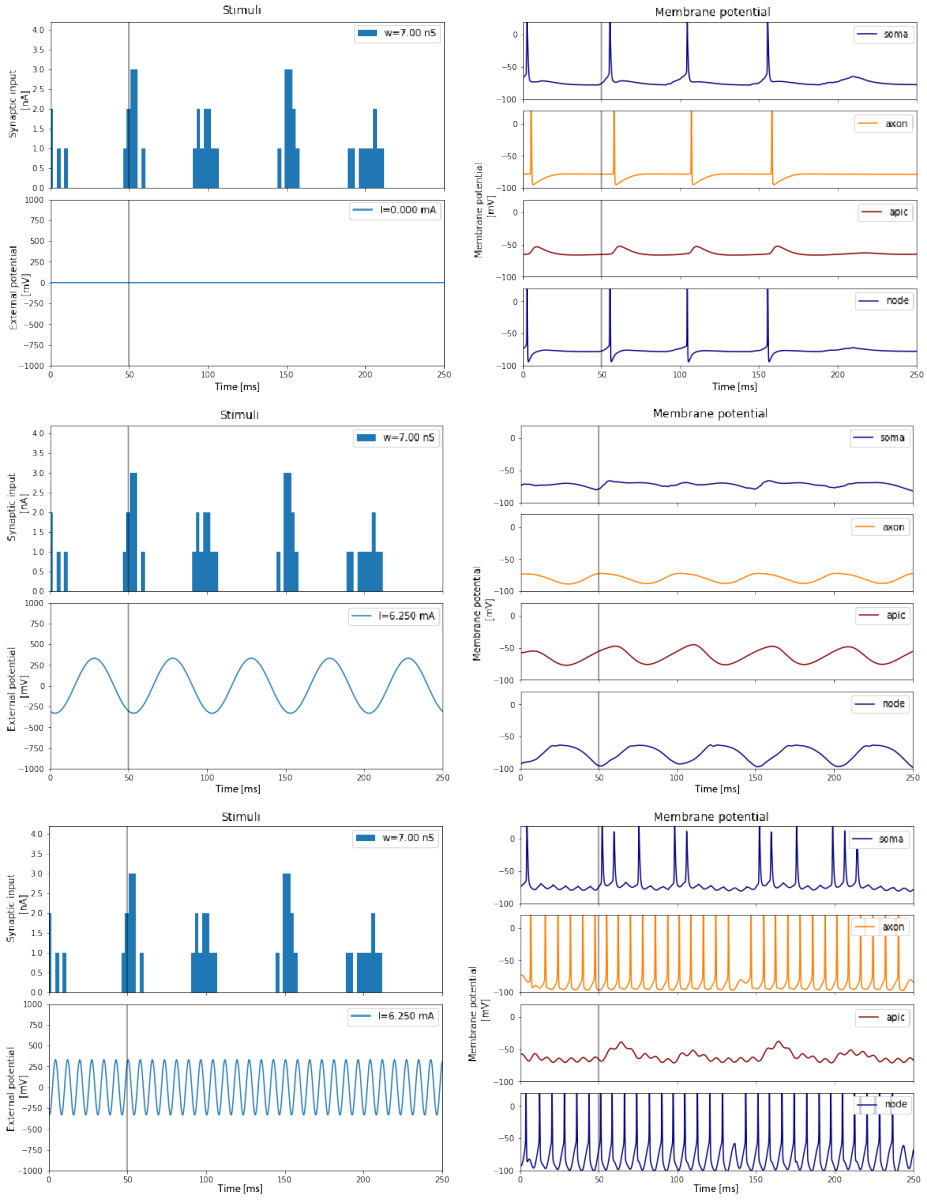

Figure 4.2: The parkinsonian neuron with and without stimulation. The membrane potential is measured at four points: in the soma, in the upwards axon, in the highest point of the apical dendrites, and the lowest axons; these are plotted in the middle column. TOP ROW: Untreated neuron with 20 Hz synaptic input. MID ROW: Neuron treated with low-frequency stimulation (20 Hz to match the synaptic input). The membrane potential is altered so that no action potentials are fired. BOTTOM ROW: Neuron treated with high-frequency stimulation (130 Hz). The treatment triggers rapid spiking in the axons, which leads to a higher but less regular activity in the soma.

4.3 Stimulation Strength

To stop the spiking completely, the strength of the stimulation has to be sufficiently strong. There seems to exist a "therapeutic window" where the current is strong enough to mostly stop the firing, but above a threshold the electrical field itself starts to induce spiking in the cell (figure 4.3). The therapeutic effect of low frequency stimulation can therefor be said to come from the sub-threshold oscillations. When stimulated with currents above threshold, the spiking adapts to the frequency of the stimulation. For very high amplitudes spikes can be triggered on both rise and fall in the sine wave, setting the spiking rate to the first harmonic of the stimulation frequency. In the Hallermann-model we found the upwards directed axon to fire on the down slope of the stimulation, while the up slope set off AP in the lowest axon. Strong stimulation could therefor entrain the neuron activity and possibly worsen tremors. The effective values seems to fit well with the magnitudes that are used in experiments and that are considered safe ([Cog+16]).

When the neuron has an axon directed towards the stimulation electrode, the neuron becomes more sensitive to the stimulation (figure 4.3). The most effective treatment is reached with a lower stimulation current, but the neuron is also adapts to the stimulation at lower current. The quenching of spiking seems to be more effective, ie. more spikes are stopped, with the directed axon.

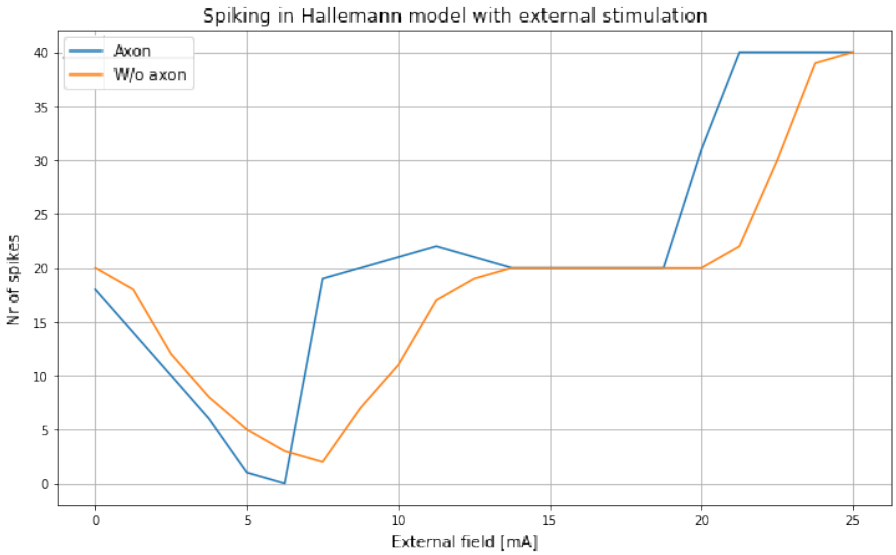

Figure 4.3: When increasing the strength of the stimulation we found a "theraputic window" before the activity of the neuron was entrained to the first and second harmonic of the stimulation frequency. The neuron is more sensitive when it has an axon directed towards the electrode, ie. it reaches the lowest number of spikes with lower stimulation but firing triggered by the stimulation also comes at a lower point. The neuron with axon is the only one where firing is completely stopped. The neurons were receiving synaptic input and electric stimulation both of 20 Hz. Average of 100 simulations.

Other Fields: New York Head Model

Comparing the results of the stimulation assuming a homogeneous field and the field from the NY Head model, we found it to be less effective in the latter case (figure4.4). When increasing the stimulation strength the spiking is only slightly reduced before spikes are started by the stimulation itself. However, the increase in activity are seen first with stimulation almost twice as strong as was the case with the homogeneous field. It could be that the NY Head field should have been adjusted slightly in phase due to inaccuracies in the calculation. If the phase is a bit off, as will be discussed more in the next part, the stimulation will be less effective in stopping the AP firing.

Although we have based our simulations on simplified head models, this shows that it is very simple to combine the biophysically complex cell models with detailed head models for more realistic simulations. For unknown reasons we found the therapeutic effect of the stimulation to be reduced in this case, and did not have time to explore the head model more. A possible explanations could be that the cell model was not properly placed compared the head model. More research is needed to resolve this, and we continued using the homogeneous field in further simulations.

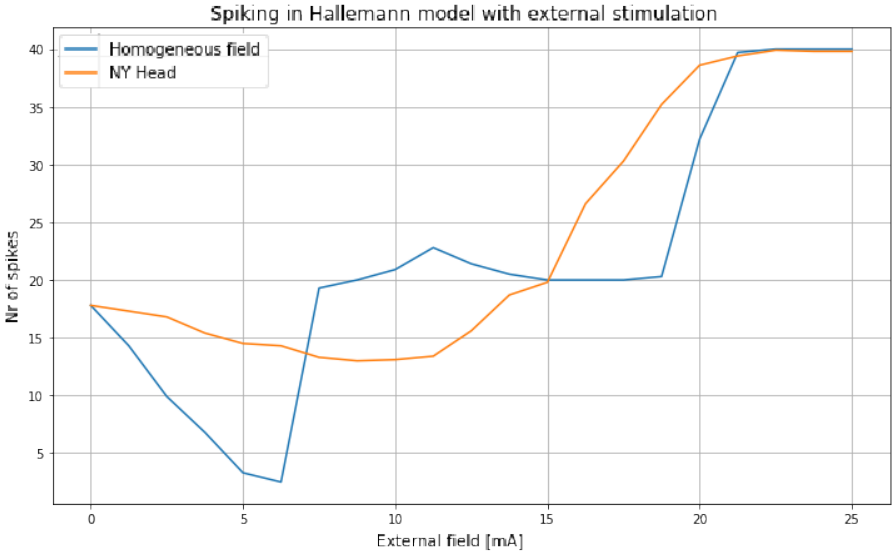

Figure 4.4: The effectiveness of the field is somewhat reduced when the more realistic NY model. The deviations from the infinite homogeneous field is more pronounced with stronger stimuli, and it affects the "therputic window". We are unsure about the cause for this, but one possibility is inaccurate placement of the cell model in the potential from the head model. Average of 10 simulations.

4.4 Stimulation Phase

The phase shift of the signal is crucial for dampening spikes. When the signal is out of phase one could be triggering additional spiking, and this could strengthen the beta oscillations. The last row of figure 4.5 shows how the aligned field can completely stop the spiking. When the field is shifted 180 degrees it reinforces the activity of the neuron as seen in the row above.

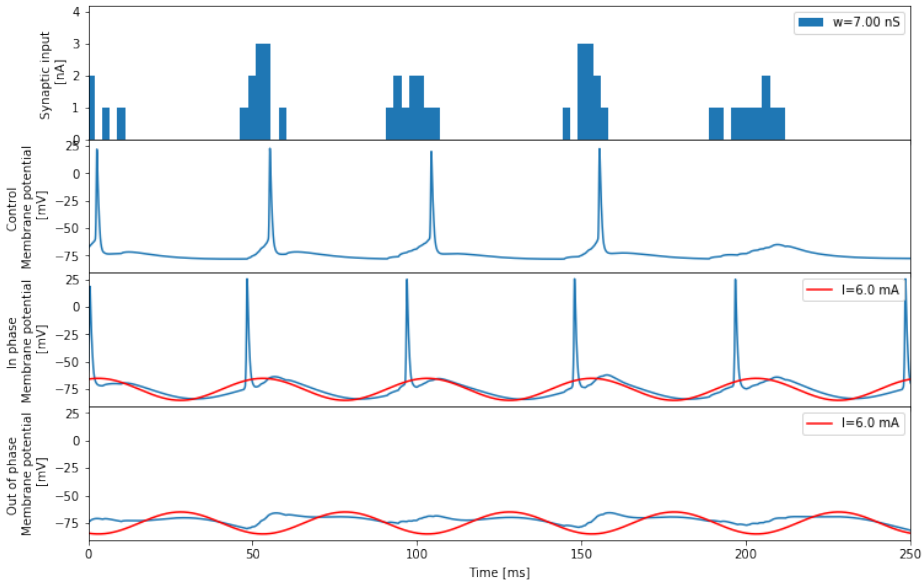

Figure 4.5: External stimulation in phase with the spiking from synaptic input to the cell exacerbate the beta-activity in the cell, while stimulation out of phase dampens the pathological spiking. First line synaptic input, second control (unstimulated) membrane potential in soma of the cell, third with 6mA stimulation in phase with the synaptic input, and fourth line with the same stimulation out of phase (shifted 180 degrees).

To stop the AP from firing, the minima of the stimulation signal should occur before the expected action potential in the soma. This sets the membrane potential so that the firing threshold is not reached. Stronger synaptic input seems to require a smaller phase shift, ie. that the minima of the signal is closer to the expected spike time (figure 4.7). The stimulation itself will shift the spike times, and this is more pronounced when the synaptic strength is weaker (figure 4.6).

Thus an oscillating neuron population with stronger connections between the cells seems to require both a stronger stimulation and a more fine tuned phase shift to be quieted.

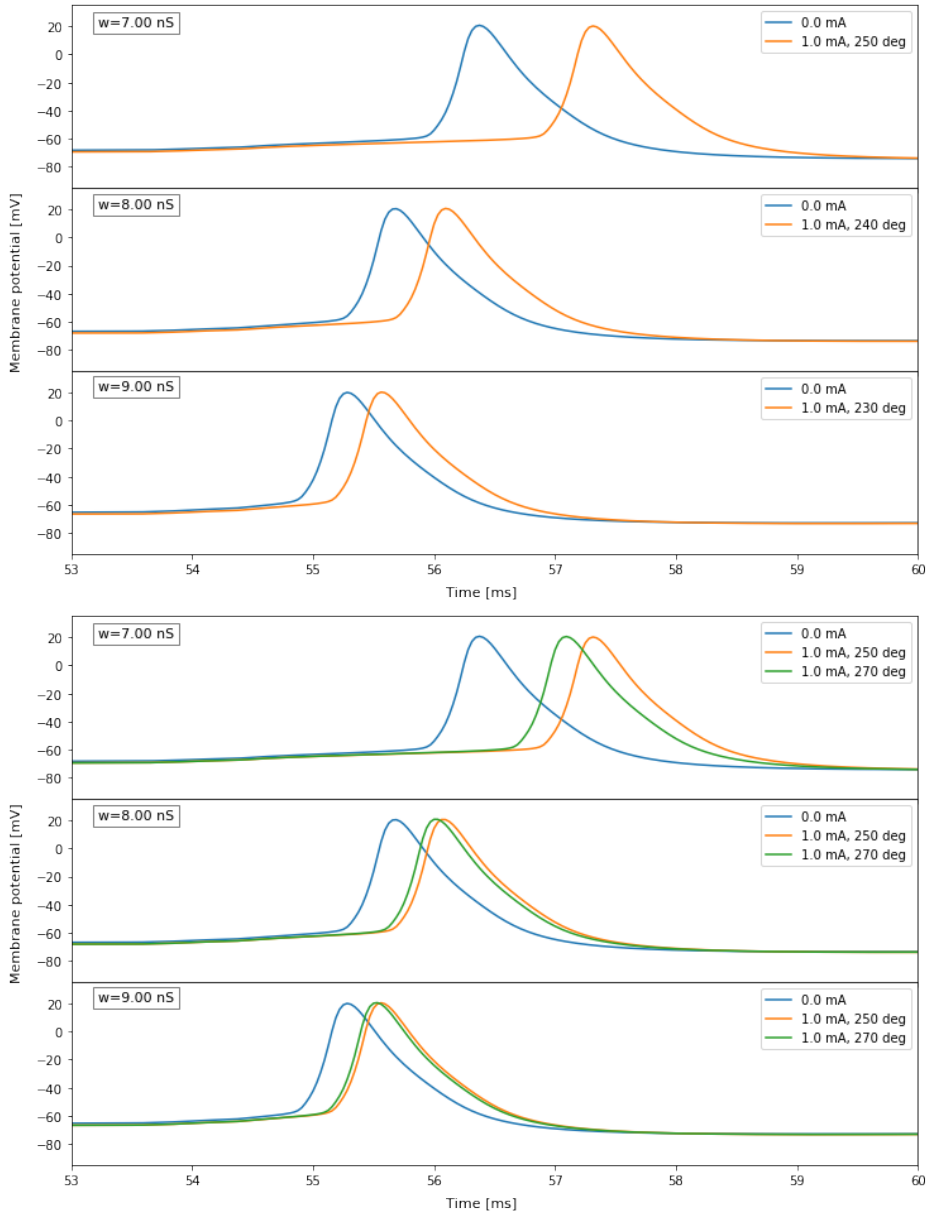

Figure 4.6: The effect of stimulation with the same phase shift on neurons with different synaptic strengths. Stimulating the cell shifts the time of neuronal firing. This could explain why the band of phases that reduces spiking are slimmer for the cells with stronger synaptic input. (figure 4.7) TOP: Neurons with different synaptic connections (7.0, 8.0 and 9.0 nS) are stimulated with the phase giving minum spiking (250, 240 and 230 degrees; see figure 4.7). The spike is shifted less for the stronger connections. BOTTOM: When stimulating all three neurons (same synaptic weights as above) with equal phase, the spikes are shifted more when the synaptic strength is weak.

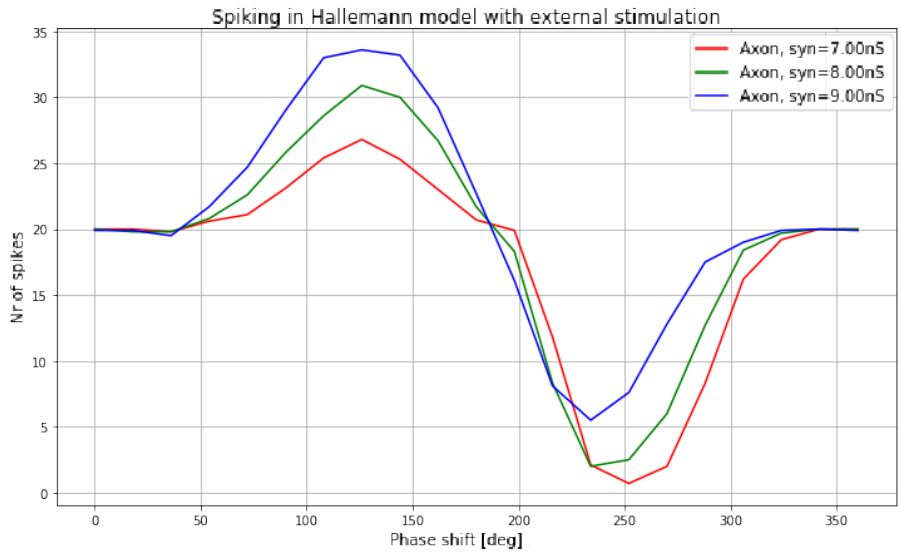

Figure 4.7: In neurons with stronger synaptic input, the stimulation has a smaller range of phases that can dampen spikes in the neurons. The phase giving the most effective dampening is also moving closer to 180 degrees for increasing, i.e. the stimulation minima has to be closer in time to the expected spike in order to stop it. Averaged over 10 simulations.

4.5 Stimulation Frequency

The dampening of spikes is most effective when the stimulation frequency matches the neuronal activity (figure 4.8 shows this for 20 Hz). Frequencies above this sets of more spiking in the neuron, but the effect flattens out. Here, neurons with a directed axon starts to fire many more APs, but this will in part be due to the neuron being more sensitive to the same current strength as we have seen above. Triggering more spikes is used in high frequency stimulation; the flattening of the the curve could mean diminishing returns for increasing the frequency. In the neuron without the directed axon $100Hz$ stimulation would not be able to disrupt the beta oscillation, so frequency would have to be increased or stimulation be strengthened for effect.

As far as we know, no experiments have been able to successfully treat the beta oscillations with same frequency stimulation; we will come back to this when discussing the circuit model. The most effective treatment seems to follow the frequency of shaking in the patients, which is much lower at about 5Hz ([Hol+18], [Bri+13]). The effect of the stimulation were reduced when increasing the frequency above this, long before reaching 20 Hz. One possible explanation could be that although beta frequencies can measured in the brain of PD patients, there could be other frequencies that affects the tremor.

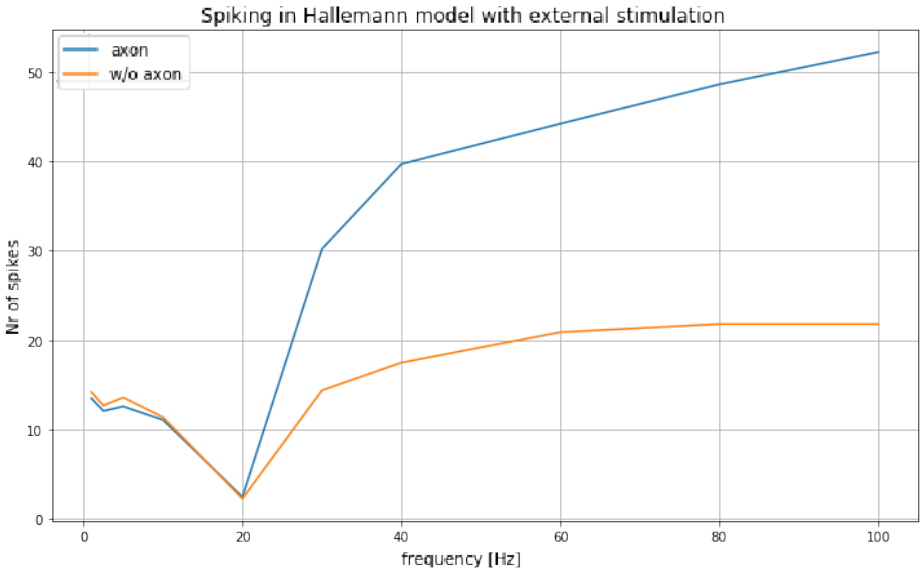

Figure 4.8: Stimulating with the same frequency is the most effective. Higher frequencies induces spikes in the neuron. Again, the upwards axon in the Hallermann neuron makes the neuron more sensitive to the stimulation by firing more at the higher frequencies. Averaged over 10 simulations.

In the Hallermann neuron, the axon directed upwards (closest to the electrode) has a peak response to stimulation of about 20 Hz (figure 4.9). The node located furthest away from the stimulation responds stronger to higher frequencies, and peaks around 100Hz. This could be the reason for action potentials firing from the bottom axon when the cell is subject to high frequency stimulation; this site becomes more polarized than the rest of the cell. The compartments on top, the apical dendrites and the directed axon, seems to be responsible for modulating the membrane potential when low frequency stimulation is applied.

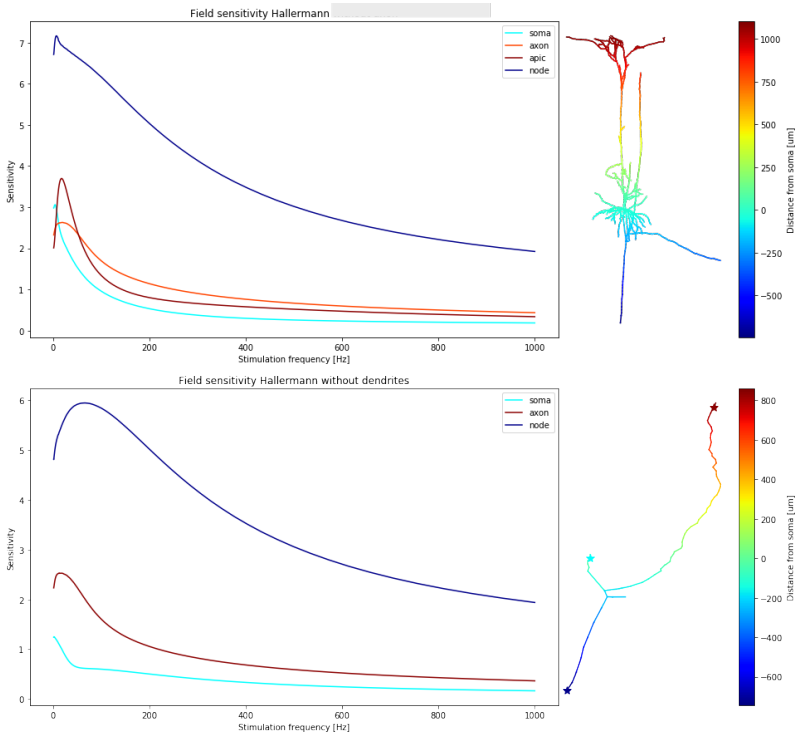

Figure 4.9: UPPER: Frequency response in the Hallerman model. The response is measured by measuring the amplitude of the membrane potential during subthreshold oscillations of varying frequencies. LOWER: Frequency response in the Hallermann cell when only the upwards directed axon, the node at the bottom and the soma remains. The top axon resonates with frequencies around 20 Hz, while the node resonates at higher frequencies, about 100Hz. The sensitivity to lower frequencies seen in the upper plot is reduced.

4.6 Stimulation Shape

We ran the simulation with differently shaped signal for the electrical field. Square pulses were not able to dampen the spiking in the model at all, but when out of phase it triggered spiking. Triangular pulses on the other hand could reduce the spiking to the same degree as the sine wave, but did not induce spikes when out of phase.

Square pulses make an abrupt change in the membrane potential. This is good for starting APs in the axons, as we saw with the high frequency stimulation earlier. They are on the other end not able to stop the APs in soma. It could be that this requires a larger reorganizing of the ions in the neuron than starting spikes, and that this requires longer time with change than the square pulses provide. The square pulses have poor performance in stopping the oscillations by quenching activity in the neurons, but could well be used if the goal is to introduce noise and disrupt the regular neural activity (mechanism of high frequency stimulation).

Triangular stimulation on the other hand leads to a more gradual change

in the membrane potential. This stimulation seems to be too slow to trigger action potentials in the cell, but is good at stopping the firing in soma. It seams reasonable that the slow change in potential gives a larger time span so that the ions can have larger reorganization and therfor stop firing. The local changes (in axons) are however not abrupt enough to start an AP. The slowly altering signal has a greater effect on the (distal) dendrites, where the hyperpolarization-activated channels (I_H) are located in high densities. These channels have a slow opening mechanic, and the current that passes through tries to can attenuate and slow down the signals moving from the dendrite to the soma, and acts like a low-pass filter for the activity ([Bie+09], [Kol06]).

The sinusodial wave falls somewhere between these two extremes, and can be used both to stop and start action potentials.

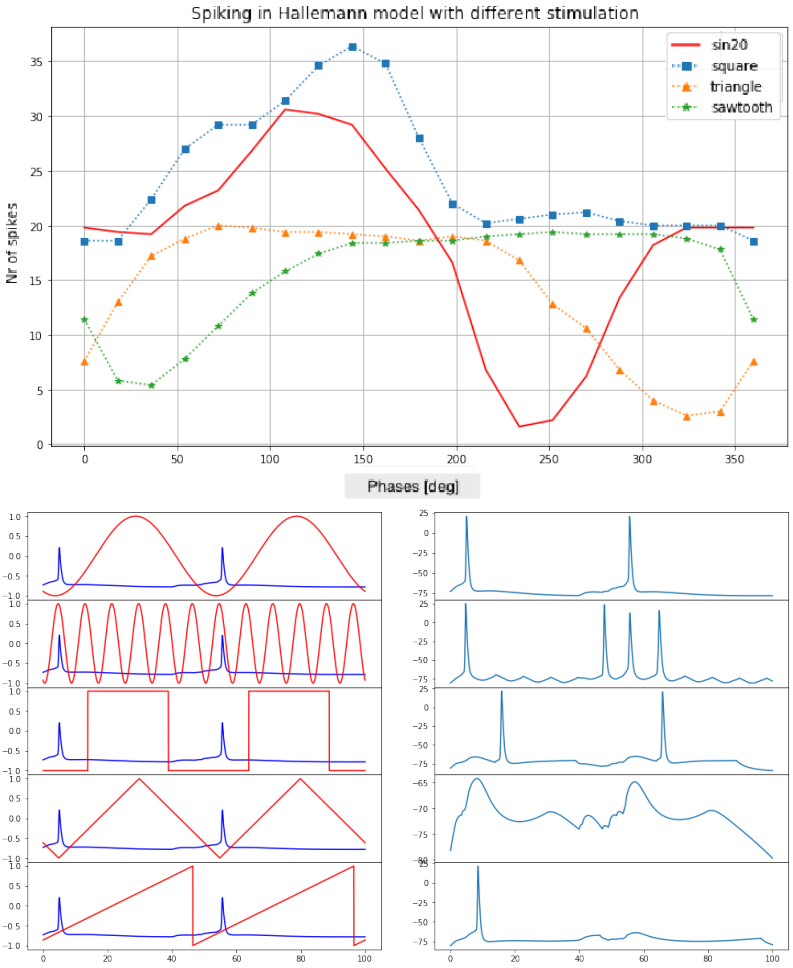

Figure 4.10: Stimulating at 20 Hz with signals of different shapes can have different effect. Slowly increasing signals are not able to trigger spiking in a cell but can stop spiking. Signals with sharp increase are much less effective in stopping spikes. However, they are good at triggering spikes, which can be used for introducing irregular firing and reduce the synchronicity.

4.7 Closed-loop Stimulation

Moving towards a closed-closed loop stimulation, we illustrated how this works by finding the frequency and the phase of the neural spiking and use that in the stimulation of the same population. To do this, we recorded the EEG and calculated from it the frequency and phase of the signal. We then ran the simulation with external stimulation with the measured frequency and the phase with a shift, and again recorded the EEG. The spiking were mostly stopped and the beta-oscillation quenched, as can be seen in figure 4.11. If the activity of the population were a bit irregular, for example by occasional shifts in the oscillation phase, the frequency and phase would have to be calculated and adjusted in tandem with the stimulation.

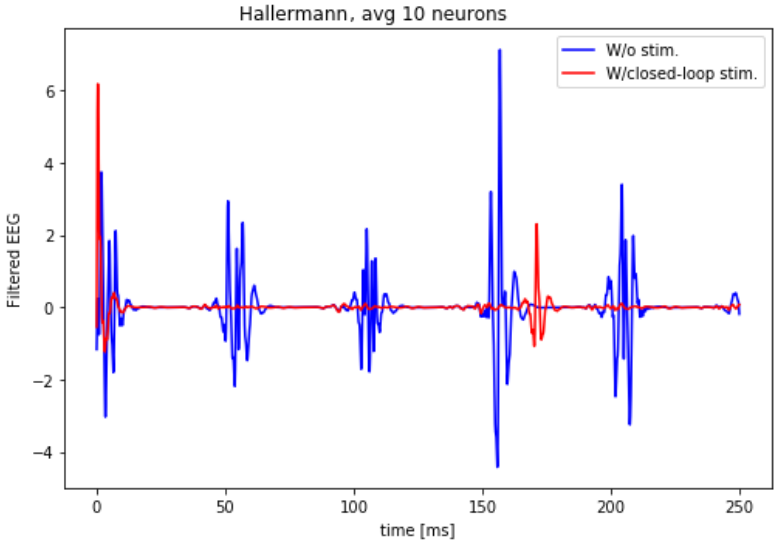

Figure 4.11: EEG recorded with and without stimulation. The stimulation was set by calculating phase and frequency from the EEG of unstimulated activity, in a closed-loop manner.

4.8 Point Source Approximation

If the cells that we wish to stimulate are sufficiently far away from the electrode, the current source can be considered a point source. According to Cogan et al. ([Cog+16]), the limit for this is about $50\mu m$. This result should however depend on the size of the electrode ([Nes+15]). When we checked this in the simulation, there is little deviation at long distances (trans-cranial lengths). From about $2000\mu m$ however, the deviation becomes larger (figure 4.13). This seems to be due in part to the neurons extension; the soma is placed $2000\mu m$ away from the electrode, but the dendrites are much closer. For trans-cranial stimulation and measurements however, this is a perfectly fine approximation.

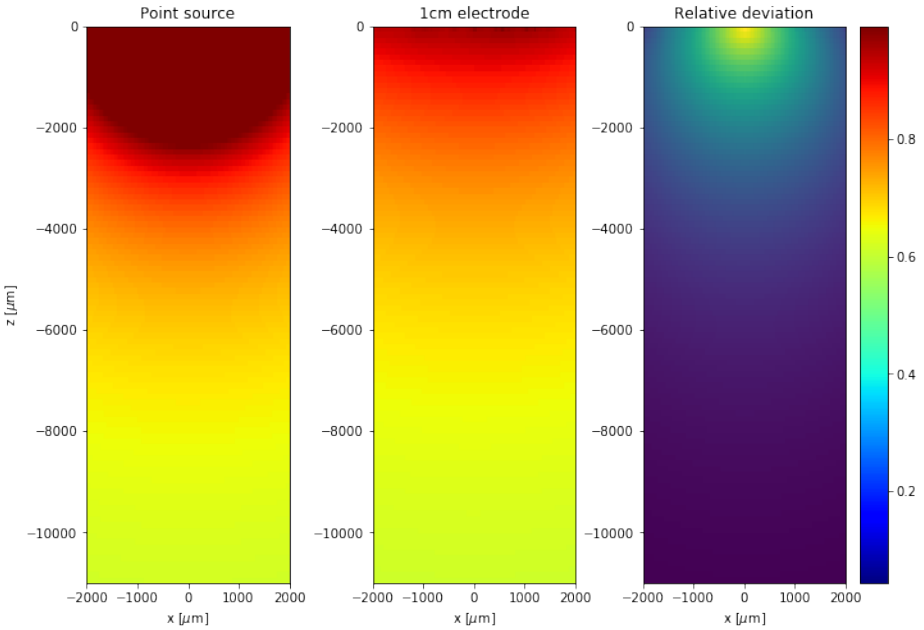

Figure 4.12: The strength of the field for the point source approximation compared with an electrode with 1cm radius. At the distance $10,000\mu m$, the distance between the scalp and the cortex, the deviation is $21mV$ or roughly 6% of the potential from the electrode at the same site and therefor negligible.

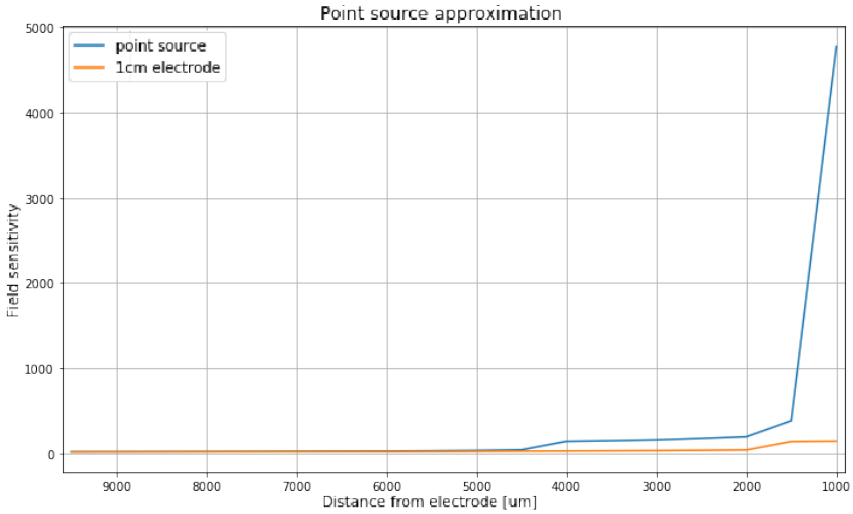

Figure 4.13: Point source approximation of an electrode. The approximation is good up to a very short distance, where the cell model starts to overlap with the current source.

4.9 Network/Circuit Model

Looking at the activity of the single cell is well and good, but Parkinson's is not a disease in cells; it is a system disease where multiple regions of the brain seems to be affected. With models for this scale, the trade of between physical details and computability typically leans to the latter. However, a physically detailed model might not be necessary for capturing the larger scale behaviours.

When tuning the network to exhibit healthy and parkinsonian behaviour under set conditions, we found that this could be fulfilled by many configurations. We have chosen to just study these, based on the "dimmer-switch" model. It could be the case that the different models respond differently to treatment. This could be studied further by finding a selection of model that satisfies the same set of criteria. This defines a parameter-space that can be studied as a whole, as Bahunga et al. did with their BG-model ([Bah+17]).

We found that by setting the connections within the STN to 0 ($w_9 = 0$), the circuit would only oscillate when the larger circuit was closed ($w_{15} \neq 0$). This behaviour is what we would expect from the third type of Parkinson circuit (cortico-thalamo-BG driven). It is therefor possible for this circuit to start oscillating by changes in the striatum-activity.

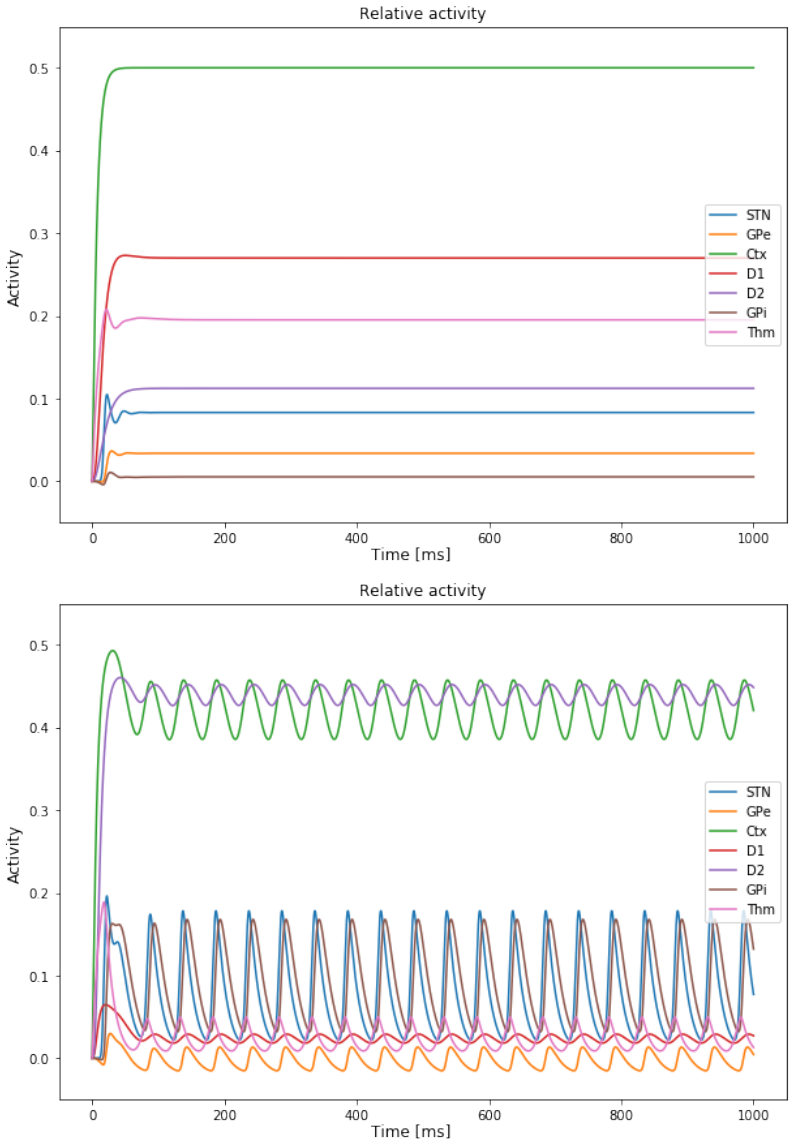

Figure 4.14: A healthy and a parkinsonian state of the model. The system is moved from one state to the other by changing the weight between cortex and the D2 population in the striatum.

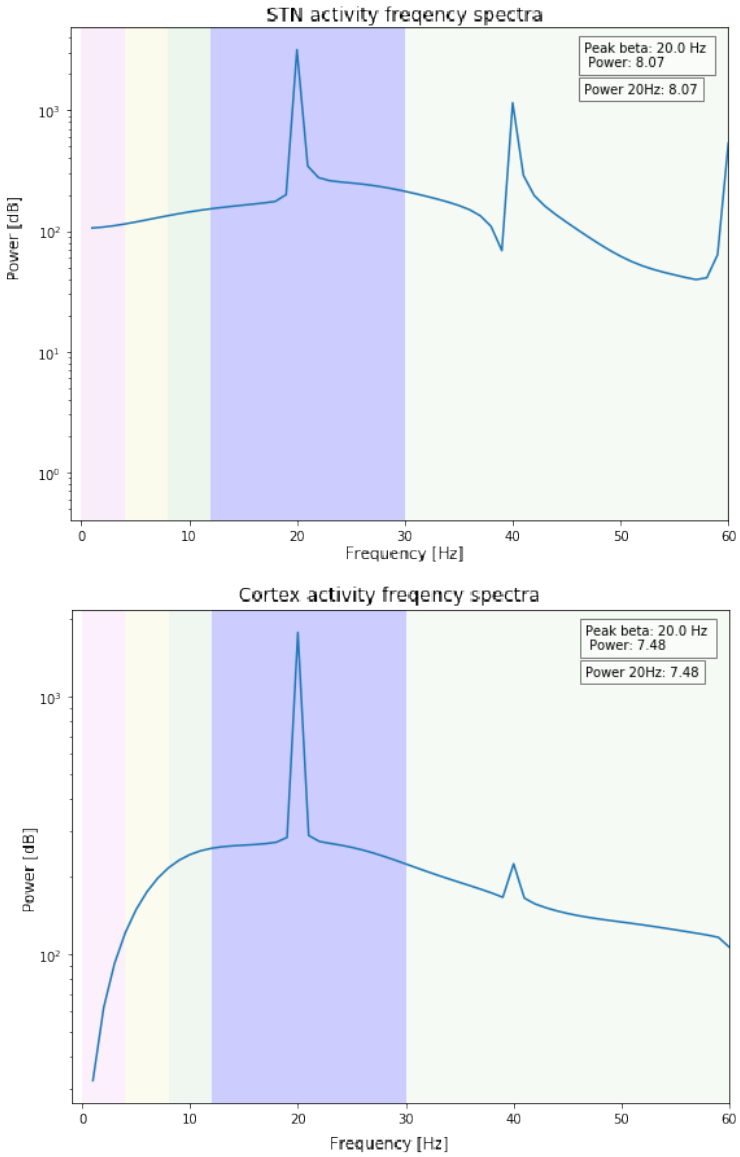

Figure 4.15: The two plots gives the frequency power spectra for the parkisonian states. The plots shows a strong peak at 20 Hz, which can be seen in the STN (left plot) and cortex (right plot).

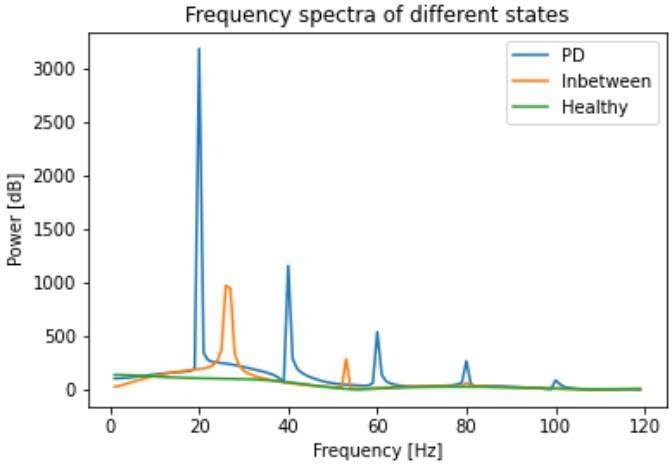

Figure 4.16: Frequency spectra of the healthy state ($w_2 = 4.0$), an "inbetween" state ($w_2 = 8.0$) and the parkinsonian state ($w_2 = 13.0$ of the model. The parkinsonian state has strong spikes at 20 Hz and its harmonic frequencies. The inbetween state has some weaker spikes shifted towards slightly higher frequencies ($26Hz$), before the spikes disappears in the healthy state where the spectra is flat.

Our model supports the hypothesis that beta oscillations in the basal ganglia can be caused by the altering of activity in the striatum, either by "removing" the compartment ($w_x = 0$) or by stimulating it with high frequencies.

Similarly to the model by Yousif et al. ([You+20]), which has a slightly different composition, the oscillations in our model are lead by thalamus and followed by cortex, STN, GPe and GPi. The activity of cortex and GPi are not in opposite phase, which Bahunga et al. found in their parameter space [Bah+17], but they are far removed, and changes to the delays between populations (τ_p) could possibly change this.

When the model oscillates, some of the populations activity sometimes goes bellow zero. Negative activity does not make much sense, but if we assume that in the resting state of the populations (zero activity) there could be some background activity that we have not included. In this case the negative activity would just mean the population is less active than in resting state.

Noise and Stability

White noise was introduced to the system in order to evaluate its stability. With smaller amounts of noise, the oscillations are able to sustain and the limit cycle is not broken (figure 4.18). The noise causes some imperfections, that are visible in the cortico-thalmo activity (right column figure 4.18), but this is not very visible in the basal ganglia (left column figure 4.18). If the noise becomes to prominent, in this case 1.5 a.u. or 36% of the average level of normal input, the limit cycle is broken and the oscillations are no longer able to sustain (last row figure 4.18, figure 4.17)

The same goes for noise introduced to the thalamus; if the noise is sufficient the limit cycle breaks down (figure 4.19). We found the oscillations to more dampened, and not just disturbed, when the noise was given to the thalamus instead of cortex. The level of noise for this is lower (0.5 a.u. or around 15% of average normal input). This makes sense as the thalamus has a lower input normally, and the connection from thalamus to cortex is necessary for driving the oscillations in this model.

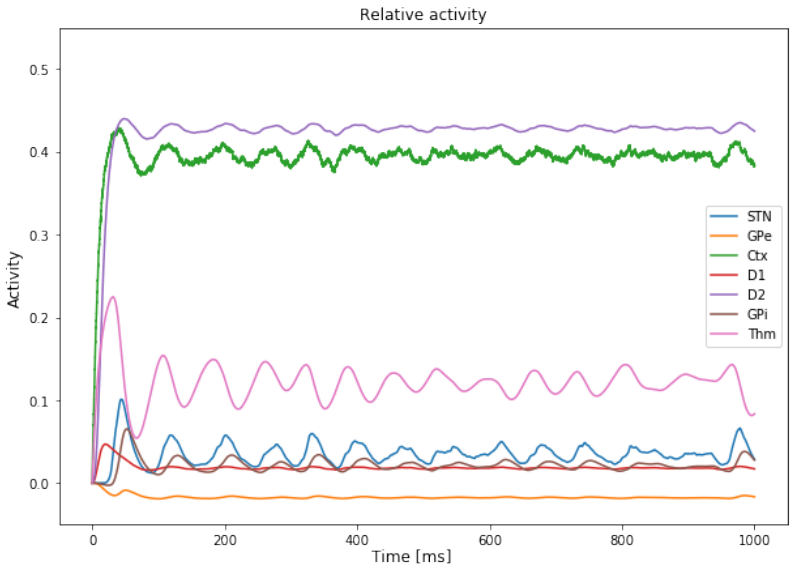

Figure 4.17: The oscillations are not sustained when the noise is too high. When the limit cycles are disrupted, the oscillations are not sustained.

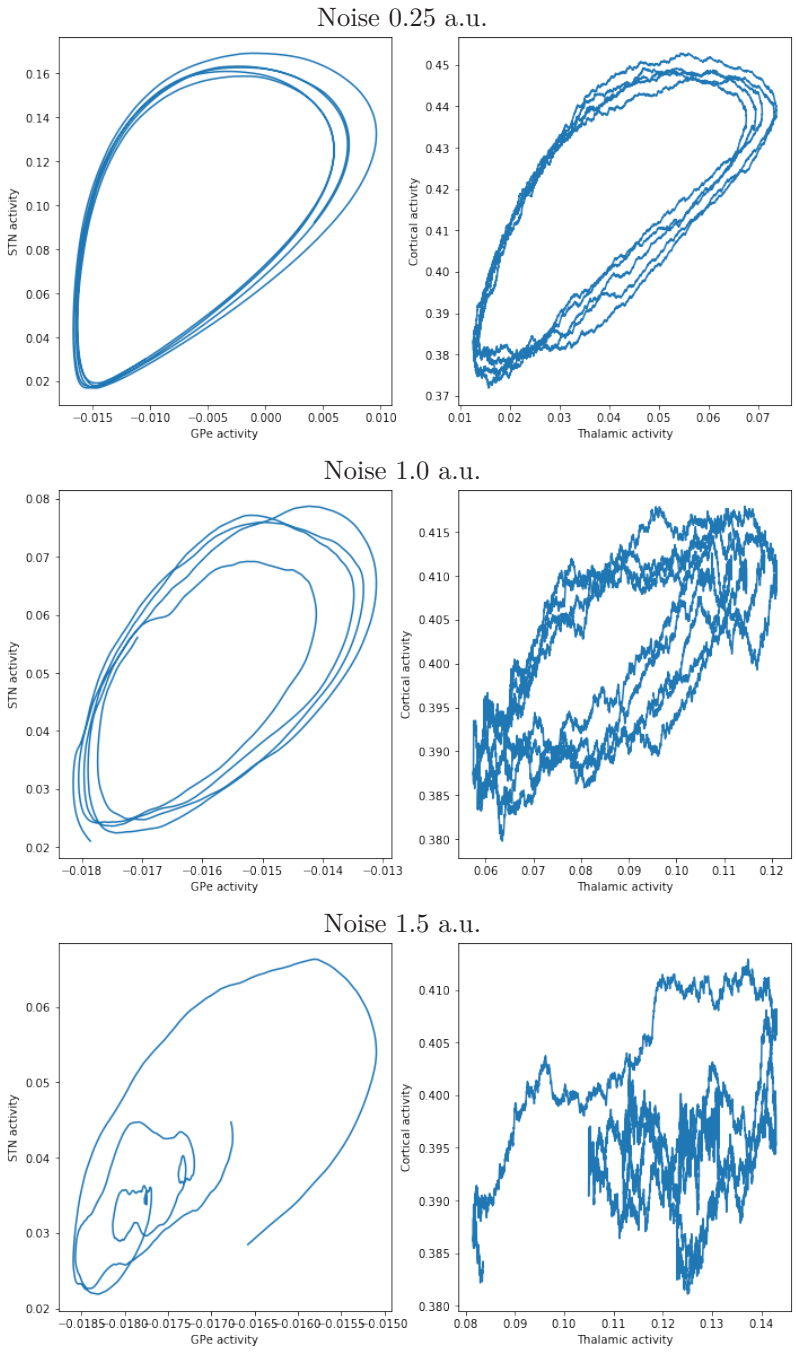

Figure 4.18: Limit cycles when white noise is introduced to cortex. UPPER ROW: wn=0.25, the activity between cortex and thalamus has some deviations, but the STN-GPe activity is intact. MID ROW: wn=1.0. LOWER ROW: wn=1.5, the limit cycles are broken. Average synaptic and external input to cortex in the PD case is 4.14.

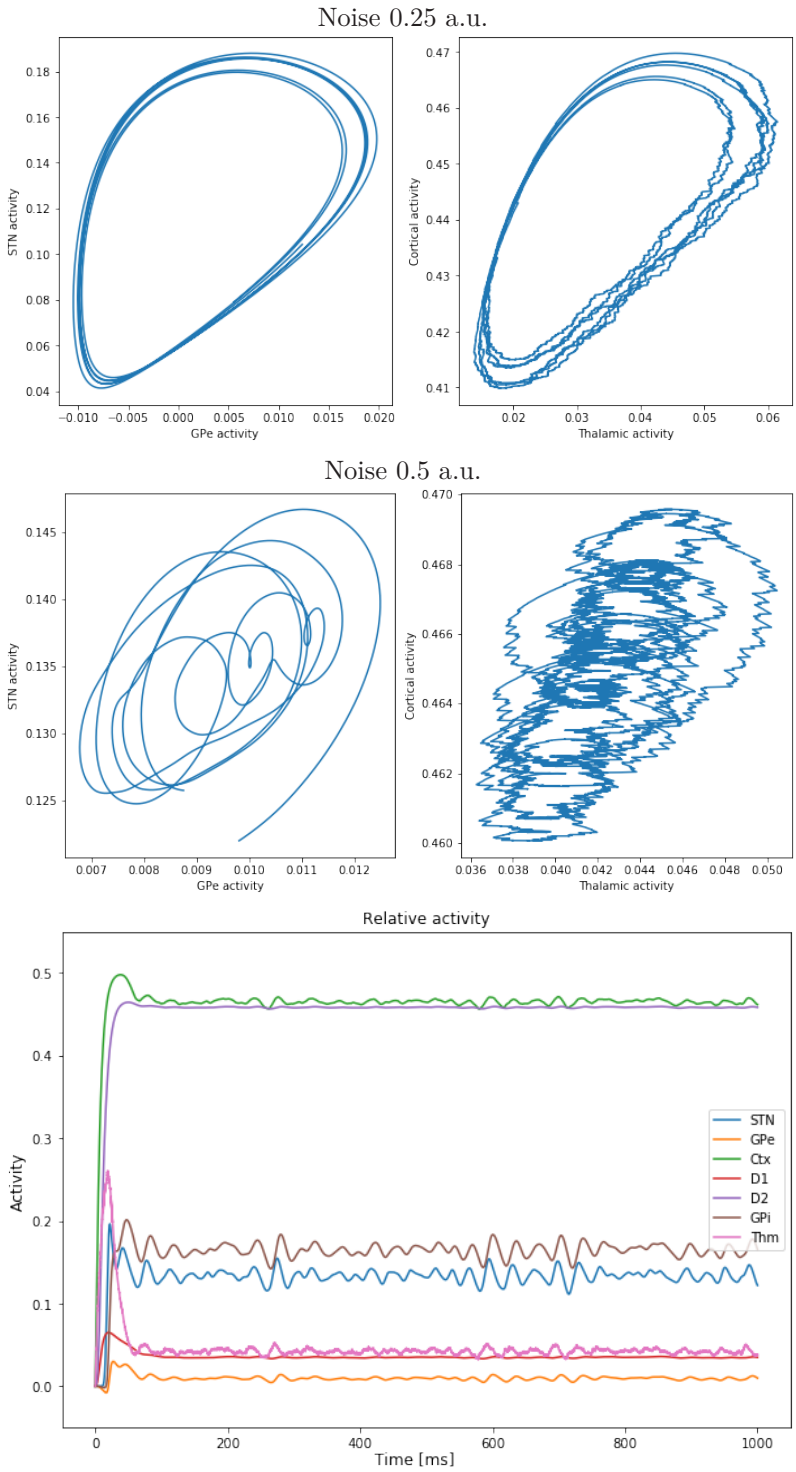

Figure 4.19: Limit cycles when white noise is introduced to thalamus. UPPER: wn=0.25, the activity between cortex and thalamus has some deviations, but the STN-GPe activity is intact. MIDDLE: wn=0.5, the limit cycles are broken. LOWER: wn=0.5, O oscillation are not sustained. Average synaptic and external input to thalmus in the PD case is 3.43.

Deep Brain Stimulation

High frequency deep brain stimulation delivered to the STN is effective in disrupting the beta-oscillations in our model. When the amplitude of the stimulation is increased to a threshold level, the beta oscillations become less dominant in the signal, and at some point they are completely quenched. The system continues to oscillate at the stimuli frequency, but the amplitude of this is lesser than that of the original oscillations. Activity in the thalamus and cortex are however reduced compared to the healthy state, suggesting that the treatment might not be helpful for treating other Parkinson symptoms like bradykinesia. The output of GPi acts as the "go" or "brake" signal for thalamus, and we take it that an increase in this with the following decrease in thalamic activity could be corresponding to a lack of movement. This is in disagreement with some experiments where DBS have had the opposite effect of making patients more impulsive ([Cag+19], [BAK15]). On the other side, if the stimulation strength was too weak, it would cause a short interruption to the activity before it glided back to (nearly) the initial state. I

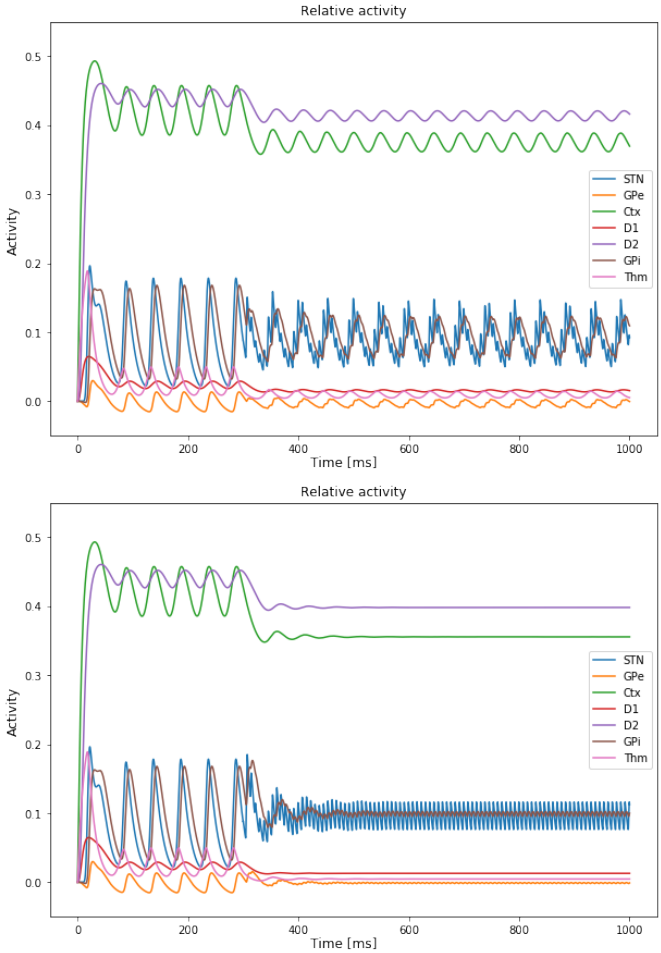

Figure 4.20

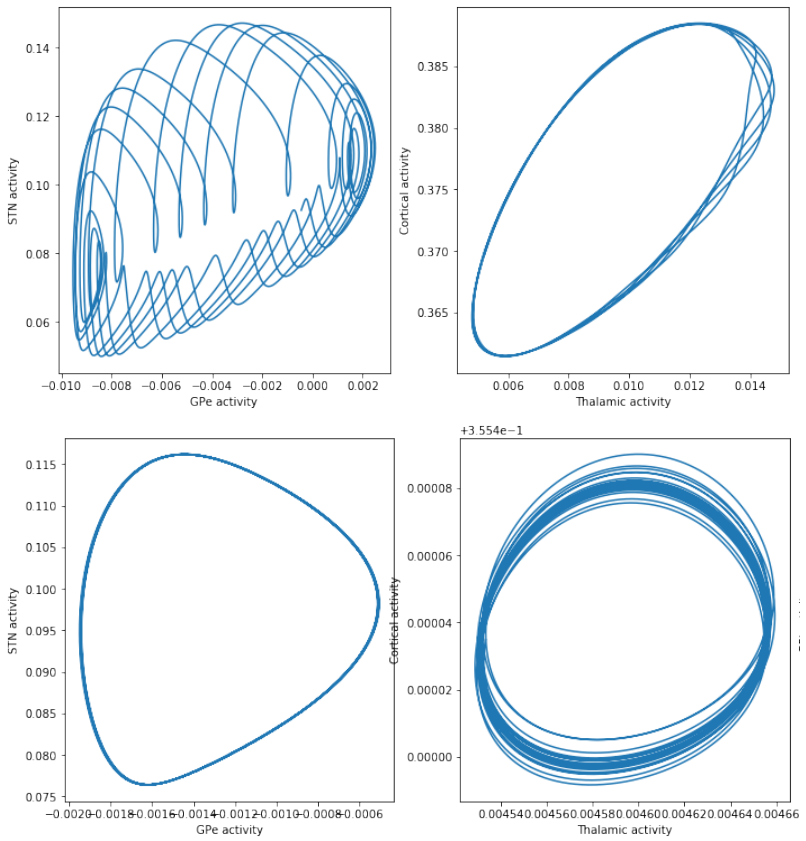

Figure 4.20: The 20 Hz oscillations are reduced with high frequency stimulation. When the stimulation is sufficiently strong (right hand) the beta oscillations decay and only the high frequency remains. The stimulation is turned on at 300ms. UPPER LEFT: Amplitude of the beta oscillations are reduced with stimulation of 0.75 (a.u). LOWER LEFT: The regular activity between populations are disrupted. UPPER RIGHT: Beta oscillations completely dies out with simulation of 1.0 a.u. LOWER RIGHT: A new (nearly) regular activity is achieved between the populations.

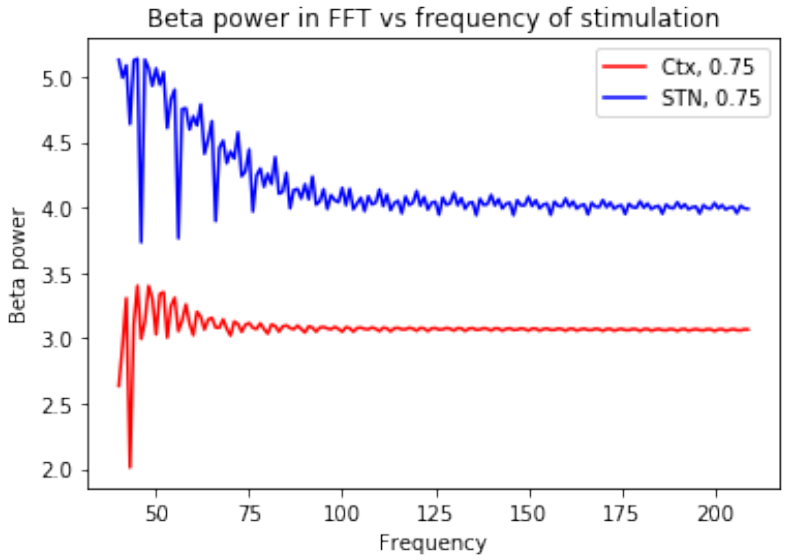

Figure 4.21: Stimulating with higher frequencies reduces the power of the beta oscillations. However, increasing the frequency has diminishing returns, so all frequencies above 100 Hz had nearly equal effect in this simulation. The stimulation strength was kept constant at 0.75 a.u..

Stimulation with "high" high frequencies (above 100 Hz) was more effective than "lower" high frequency stimulation in reducing the beta oscillations (figure 4.21). We found that increasing the frequency in general gave better results, but above 100 Hz the differences were rather small.

Stimulating with lower frequencies have little effect in reducing the oscillations. From the single cell simulations we found that low frequency stimulation works by shifting the membrane potential so that the threshold for firing would not be reached. This effect is not accounted for in the WC-model. If it were to be included, the sigmoid function would have to be altered by the stimulation, ie. a_p and θ_p would depend on the stimulation.

Stimulation with the same frequency as the systems oscillations were not very successful in our simulations. The system oscillations are entrained by the stimulation-signal after approximately one period, and the system keep oscillating at the pathological frequencies. This is similar to experiments where stimulation at beta-frequencies have not yet been very successful ([Hol+18], [Cag+16]). The circuits works like a resonator, so although stimulating with the same frequency as the initial activity is most effective at the single-cell-level, it might not work on this level. Cagnan et. al found that the tremor circuit has a broad frequency-amplitude band, ie. that a change in the frequency of the oscillation leads to only a small change in the oscillation amplitude. In order to push the system out of its resonance-behaviour, the stimulation frequency has to be relatively far from the oscillation frequency. In our model, the oscillations could be entrained by close frequencies (eg. move it from 20 Hz to 15 or 25Hz) if the strength of stimulation was high enough ($\geq 0.5 a.u.$).

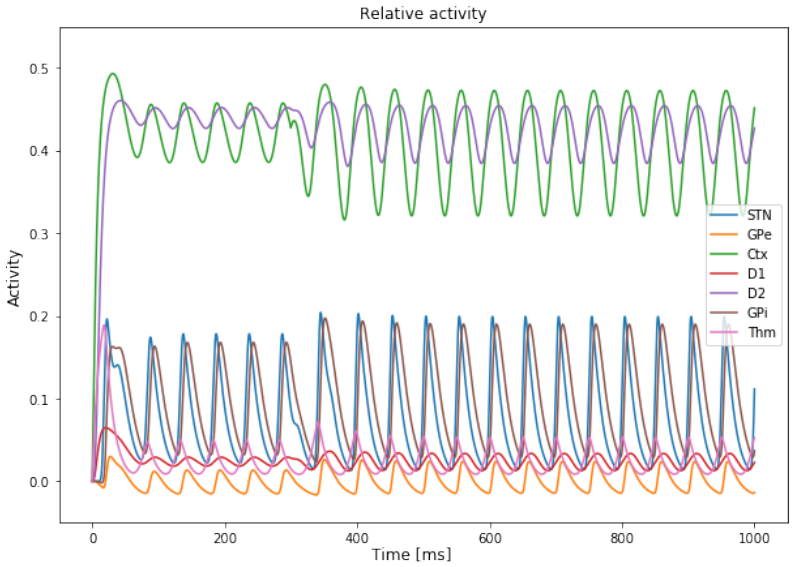

Figure 4.22: Stimulating with the oscillation frequency has the activity of the circuit adapt to the stimulation, and results in a strengthening of the pathological activity.

Trans Cranial Stimulation (TCS)

It is possible for stimulation of cortex to affect the downstream basal ganglia populations. This is however dependent on some conditions. If the oscillations between GPe and STN are self sustained, ie. they do not require oscillations or large changes in cortical activity to sustain, they will probably not be stopped by cortical stimulation. On the other side, if cortical oscillations are necessary for the oscillations not to dampen out, cortical stimulation is more disruptive. In our model, where STN-intraconnection were set to zero, the thalamo-cortical connection was necessary for driving oscillations, and not very surprisingly the STN-oscillations were reduced with (high frequency) stimulation to cortex (figure 4.23). Differently tuned models would be useful for studying this more, but our model gives a "proof of concept" that TCS could reach down and stop oscillations in the BG.

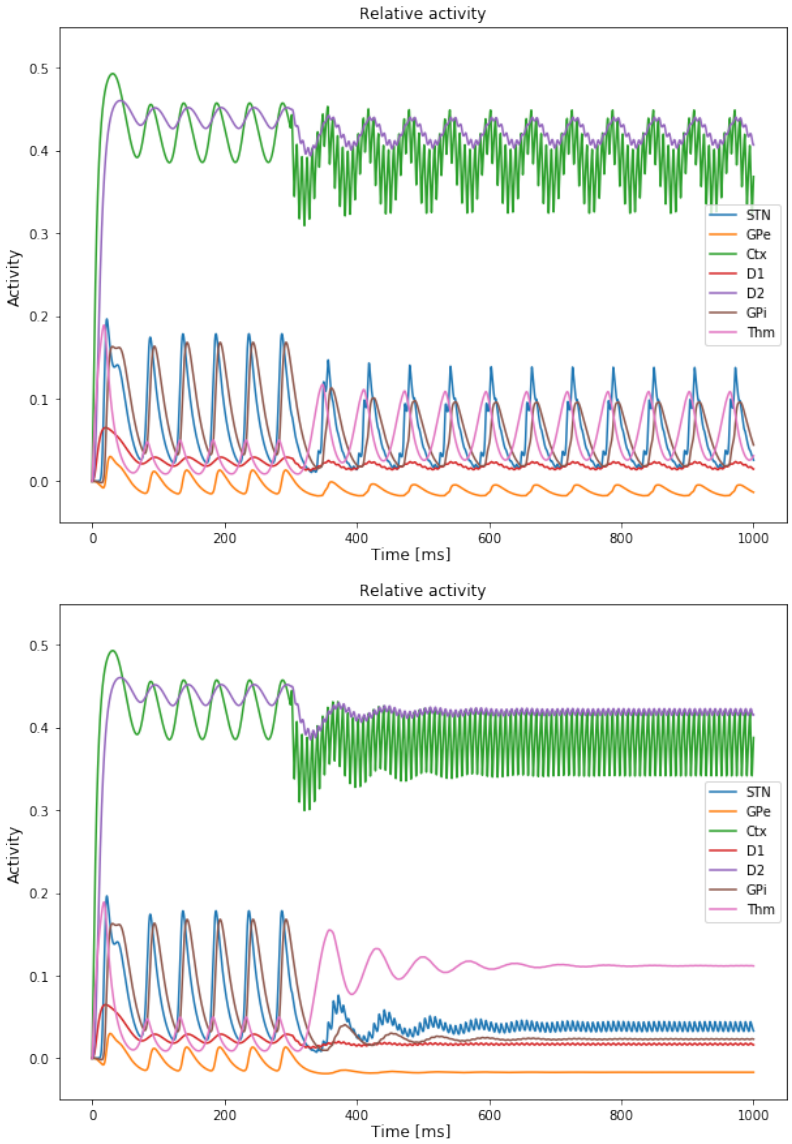

Figure 4.23: High frequency (130Hz) stimulation to cortex with stimulation strength of UPPER: 0.75 a.u., the beta oscillations are still maintained in basal ganglia but with a reduced amplitude. LOWER: 1.5 a.u., the beta-oscillations are successfully suppressed.

When the oscillations are reduced through the whole circuit, there some of the compartments still exhibits an abnormal activity level. The striatum is still affected, with higher than normal activity in D2 and reduced in D1. The reduction of activity in cortex and thalamus also remains in high frequency stimulation, and as mentioned before, this could mean other symptoms are not resolved.

Adaptive Brain Stimulation

To test our hypothesis from the single cell simulations, that treating the beta oscillations with the same frequency in opposite phase should be the most effective method, we found that in the circuit model this will in best case shift the oscillations slightly, and in worst case strengthen the beta oscillation (see figure 4.22). The circuit works as a resonator for this specific frequency. Adaptive brain stimulation were therefore tested to avoid this effect.

The stimulation is made to adapt to the activity of the STN by adjusting the phase every $50ms$ so that it is 180 degrees behind the population activity. We were not able to stop the oscillations by this approach, but the continual interruption and entrainment of the activity caused a slow down of the signal to a slightly lower frequency (still within the beta-band).

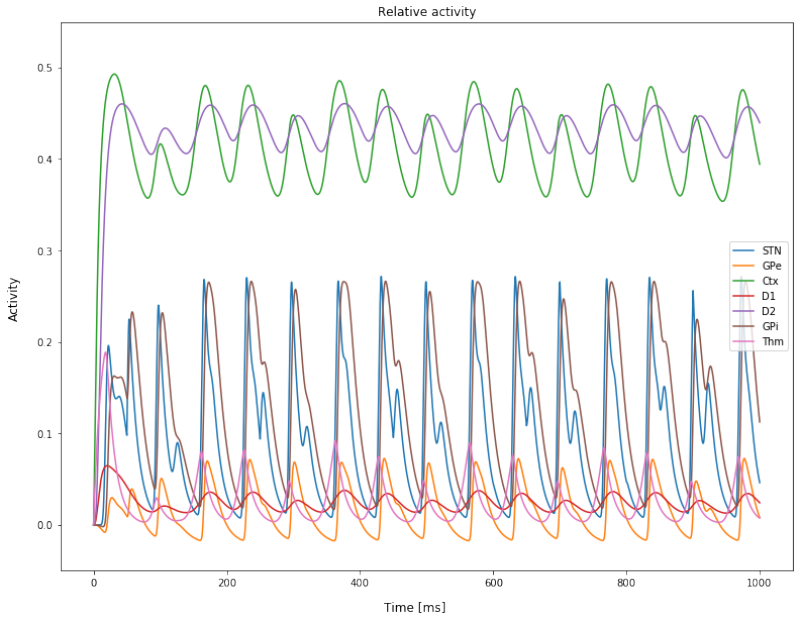

Figure 4.24

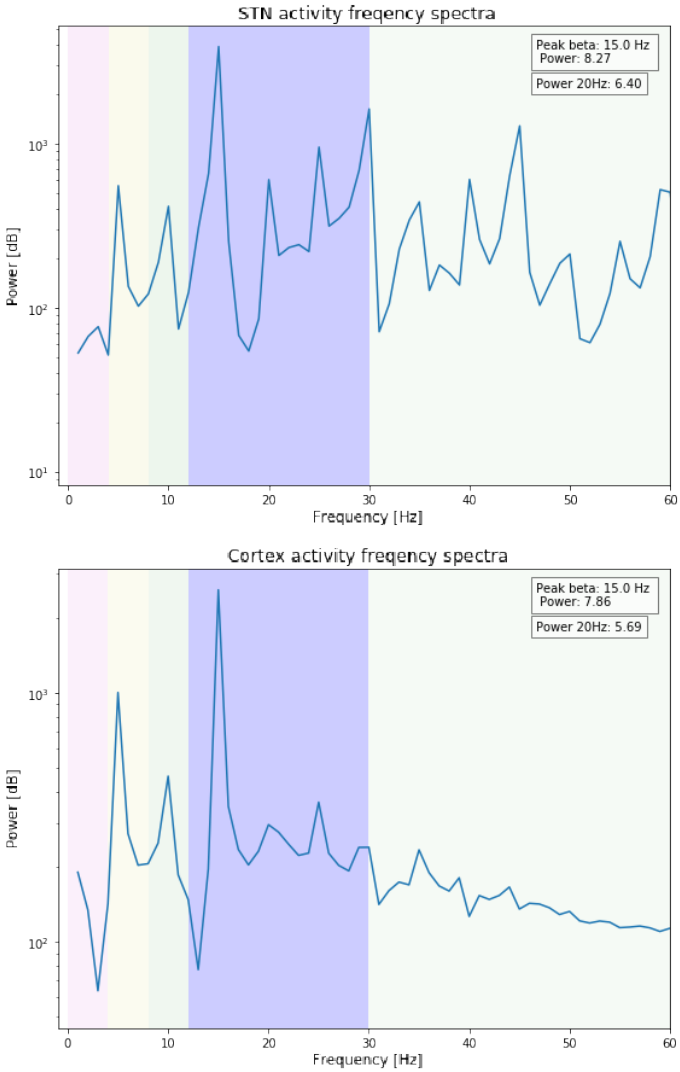

Figure 4.24: Adaptive brain stimulation. The activity of the populations adapt to the stimulation in some milliseconds. When the stimulation phase is continuously adjusted, it delays the oscillations which lowers the frequency. With stimulation strength of 0.75 a.u., the peak frequency is $15Hz$.

Taking a step back to the single cell simulations, we also looked how the adaptive brain stimulation worked on this scale when the cell is not spiking regularly, but has a shift in the phase ever few periods. This is less effective than regular stimulation to regular activity, but fares better than non-adaptive stimulation to the same neuron. We tested a couple of different periods for updating the phase, and found updating every 50 ms to be better than every 25 ms for a neuron with 20 Hz spiking (figure 4.25).

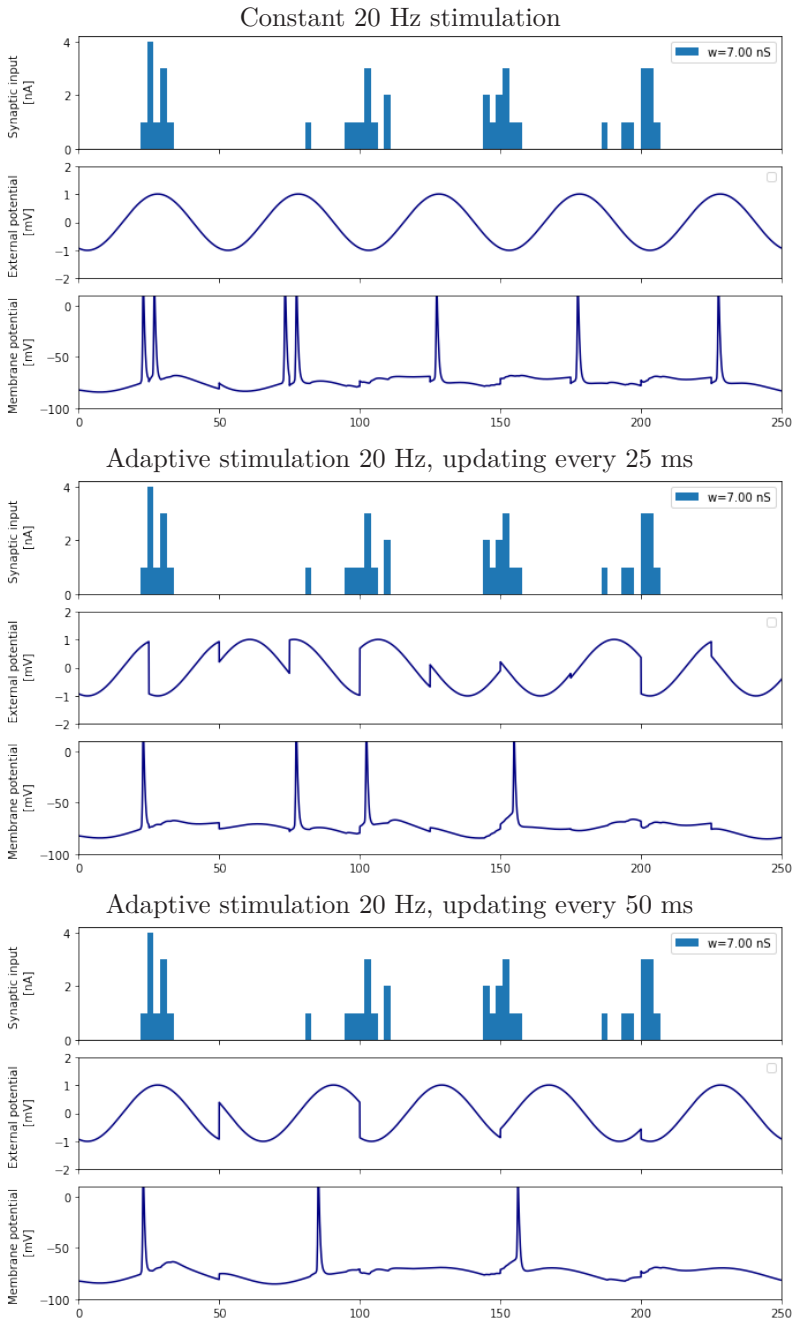

Figure 4.25: Adaptive brain stimulation for single cell. UPPER: Constant stimulation with 20 Hz. MIDDLE: Adaptive stimulation, updating every 25ms. LOWER: updating every 50ms.

Where to Stimulate

High frequency stimulation to the parkinsonian system has reduced the beta oscillations. The system, however, is not healthy. The relative activities are not where they are in the healthy state, and this could mean other symptoms are not fixed. The activity in thalamus and cortex for example are very reduced, which could mean that movement is low like in bradykinesia and rigidity. We therefor explored whether different stimulation (targeting other or multiple sites) could help.

We did not have enough time to set up and run simulations on this topic. The linearized model described under 3 could be used for exploring this, and maybe by application of control systems theory could be useful.

When we quickly looked at stimulating multiple sites simultaneously a somewhat peculiar result was that when we added high frequency (130 Hz) stimulation of 0.5 a.u. to both the STN and thalamus (0.5 a.u. is relatively stronger for thalamus than for STN), this "regenerated" the beta oscillations, which was stopped if the same stimulation was given to STN only (figure 4.26). The same was not observed if STN stimulation was turned up to 0.75 a.u.

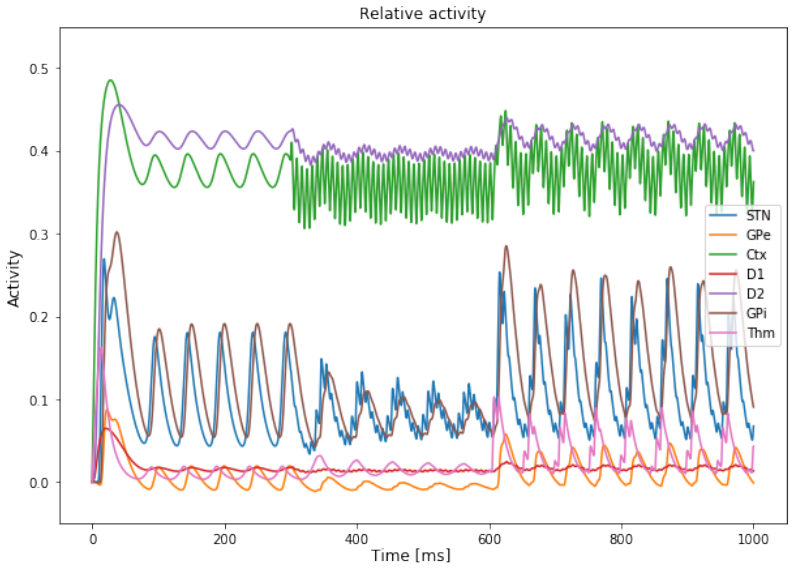

Figure 4.26: High frequency stimulation (130Hz) of strength 0.5 a.u. is sent to both STN and thalamus. Stimulation to STN is turned on at 300 ms, and reduces the beta oscillations. When the stimulation to thalamus is turned on at 600 ms, beta oscillations are strengthened again.

CHAPTER 5

Discussion

To increase the effectiveness and reduce side effects of electrical brain stimulation, for example in Parkinson treatment, understanding the mechanics of different treatment is useful. Low frequency stimulation works by stopping the targeted activity, and may therefor be more precise way of treatment than high frequency stimulation that triggers "random" firing in the neuron. However, the low frequency stimulation requires fine-tuning to be effective. When the synaptic connection between the neurons is strong, the activity becomes more rigid. The stimulation has to be in proportion to this both in strength and in phase to most effectively stop the activity. Stronger synaptic inputs are more finicky in regards to the phase.

Both the morphology, in terms of branching, of a neuron and the distribution of ion channels affects its response to the electrical field. We also saw when using the Hallermann model that having an axon directed towards the electrode made it more sensitive to the stimulation. Differences in the ion-channel distribution in different parts of the neuron makes part of the cell more or less sensitive to specific stimulation. For modulating the membrane potential, as in TcS, a slowly changing field is needed, so sine- or triangular waves are better than square-pulses. For setting off spikes, like in high-frequency DBS, square-pulses can be used.

The damaged basal ganglia might function as a resonator for the beta-oscillations. This is what we observed with the Wilson-Cowan model, and it could be one explanation as to why stimulation at the exact frequency of the pathological oscillation (or close there to) has been unsuccessful in in-vivo experiments. Cagnan et al. found stimulation at the tremor frequency, ie. very low frequency, to be most effective in treating parkinson tremor (and other tremors), and that increasing the frequency weakened the effect ([Cag+14]). The fact that tremor frequency seems the most effective could indicate that there are lower frequencies in cortex that controls the tremor, while the beta-oscillation might be more involved in other symptoms, e.g. reduced movement ([LB14]).

Adaptive brain stimulation could also help to mitigate the resonance behaviour, but in our model it did not have a great effect. Continuously changing the frequency along with the phase could possibly help, and could be interesting to study later. The Wilson-Cowan model is quite naive; altering the membrane potential the way low-frequency stimulation does is not included in the model. This might be necessary if one wishes to study the effect of low frequency stimulation, so an extended model (or a different type of model)

might be required.

In despite of this, it was possible to recreate different behaviours in the PD circuit model, like a shift from healthy to parkinsonian behaviour by shifting striatum activity, and a good response to high frequency stimulation. We were not able to create some other features of the basal ganglia. While the subthalamic nucleus has been seen to oscillate at 20Hz, the external globus pallidus is more active at 45Hz. In our model, the activity of these are following each other closely, and if the oscillation is strong enough it will be seen throughout the whole system. One way to include the different frequencies is to consider the relative activities between the population in the healthy state, and scale them by the population sizes and take this as the average activity of the population. We ran a parameter sweep to find such a model, but found none. Maybe changing other features, such as the sigmoid function, could change this, or allowing for more possible configurations. The different spike-frequencies could possibly carry interesting information, particularly about the in-between state of healthy and parkinsonian activities.

The parameter-space that can create parkinson-like tremors in the model is vast, and we have in no way exhausted the options. Different tuning could give models with different characteristics which respond differently to stimulation, and experimental data might be necessary to decide which of the possible models are more or less correct. Parkinson does not need to be a one-to-one system, where the same symptoms are created by the same degradation in the brain; the same oscillations and tremors could be created by different changes in different patients. The disease could be represented by a parameter-space, and studying models in aggregate in the way of Mirzaei et al. is a more reasonable approach ([Mir+17]) to this problem.

We have also neglected some populations in our model. Adjusting other connections is probably sufficient to account for much of this, at least in models with simplified dynamics, but its possible some simplifications affects the dynamic in a way that makes it more difficult to study the circuit effects. One of the populations mentioned earlier was the TA (arkypallidal) population in GPe. The two populations of the GPe might have very different roles in the BG; TA fires at a much lower frequency ($5 - 10Hz$ vs $30 - 40Hz$) ([Bah+17]), and they mainly target different populations. TA also inhibits the D1 neurons in the striatum, which makes GPe a part of all three pathways to the GPi. During beta-oscillations TI and TA neurons fire at opposite phase, but how exactly the TA activity is affected by PD is uncertain ([Mal+12]). In their Wilson-Cowan type model, Yousif et al. found the GPe to shift the system between oscillatory states ([You+20]). Their model only include the TI population, but it could be GPe's role in the different pathways, affecting GPi in complex ways, that causes this.

The thalamus have many sub-populations, and connections between them and cortex creates parallel circuits that might modulate the behaviour of the circuits we have modeled. Yousif et. al found this parallel circuit to affect the frequency of the oscillations ([You+20]). Although not necessary for producing oscillations, these parallel circuits could alter the activity and possibly be part of finding more effective treatments for PD.

The thalamus is often thought of as a hub that only relays information between different parts of the brain. Synchronicity of the populations in basal ganglia can cause pauses in the activity of GPi, and this can trigger "noisy"

rebound spikes in thalamus.([NRS18]). The rebound spikes normally comes after a motor signal and is part of movement control, so increased noise may disrupt movement. This is maybe not important in a simplified model like the Wilson-Cowan model, but in a more complex model this might be worth taking into consideration.

High frequency stimulation to the (ventrolateral) thalamus has been effective in reducing tremor, but do not help the rigidity and bradykinesia ([Cag+19]). This could suggest that it modulates the output activity that causes the tremor, while the beta-oscillations are created further down in the basal ganglia relatively unaffected by the fluctuating activity in the cortex.

Deep brain stimulation has a positive effect on reducing beta-oscillations during the time of stimulation, but also for some time after ([LB14]). This could be due to plasticity in the populations. Deep brain stimulation to the STN or GPi have both been shown to cause synaptic depression ([Ros+14]). This seems to be due to a combination of axonal- and synaptic failure. This is hypothesized as a remedy for the observation of increased activity in the axons during DBS, and not a decrease as one might have thought. The short term depression can help in decoupling the activity of STN and its connected populations. The reduction in beta-oscillation may thus be due to both a reduction of (pathological) activity in the targeted population and a weakening of its output connections. We found in our simulations that high frequency stimulation does trigger rapid firing in the axons. The synaptic failure could be one explanation for this, but APs failing to propagate to soma could also have an effect here. Rapid output from one cell might not be able to set of similar activity in its receiver, especially if the connections are far away from the soma.

When recording the EEG in experimental setups, the "contamination" of stimulation signal should be limited. This can be done by alternating between stimulation and recording. This is done with a higher frequency than the 20 Hz, which would probably not disrupt the treatment too much because of the inherent slowness in the system. This alternation is not required in simulations, but if the activity was "slipping" when stimulation were turned on and off, it could be good to include.

Little and Brown mentions as an alternative cause of the DBS having effect both during and between stimulation periods, that this could be due to a delay in a system with multiple coupled oscillators ([LB14]). In our Wilson-Cowan model, which do not have any plasticity, this is what we see when the system uses about $100ms$ to adjust to the stimulation.

To summarize, we have studied the possibilities to treat Parkinson's disease with the use of electrical stimulation. The pathologies in biophysically detailed single-cell models and high-level network activity both have been tried treated, and we found in both cases that the beta-oscillations could successfully be reduced. The most effective treatment contradicts on the two scales; for a single cell the ideal treatment is to stimulate with the pathological frequency, but due to resonance phenomena this worsens oscillations in the network model. We hope that this work can be helpful for gaining better insight into the mechanisms underlying the pathology and in the search for better treatments.

Appendices

APPENDIX A

More on the Wilson-Cowan Model

A.1 The Wilson-Cowan Model and Fitting the Weights

To assure that the oscillations in our circuits were created in the Basal Ganglia, we started the fitting process with only two populations, the subthalamic nucleus (STN) and the globus pallidus externus (GPe). We assumed the input to these populations, from cortex to STN and from D2 to GPe, to be constant. With this model we could easily follow the process described by Wilson and Cowan in their original paper ([WC72]) for finding a model that oscillates.

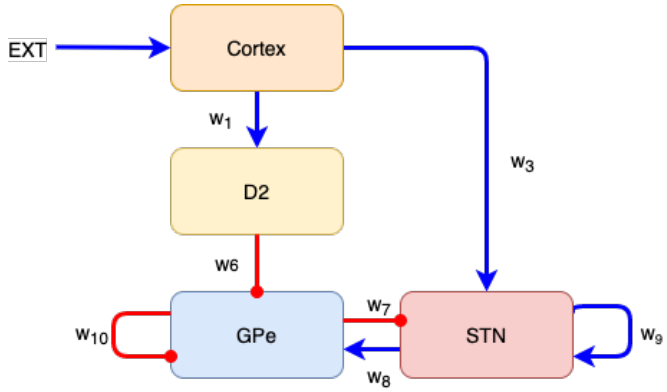

Figure A.1: The smaller circuit.

The following three criteria were laid out for a system that oscillates. The criteria is sufficient for oscillations to arise in the model, but not necessary.

$$w_9 * a_e \geq w_{10} * a_i + 18$$

$$\frac{w_7 * a_e}{w_9 * a_e - 9} \geq \frac{w_{10} * a_i + 9}{w_8 * a_i}$$

$$\frac{w_9 * a_e - 9}{w_7 * a_e} \leq 1$$

We chose to use different values for a_p and θ_p, the ... and the turning point of the curve, for the sigmoid activation function. This changes the threshold for

firing, but other values could have been use with no significant change. However, this might the relative activity of the population (or at least what values they swing around), so if this is important the specific values might be chosen with more care.

	Values used	Wilson-Cowan values
a_e	9.0	1.3
θ_e	4.0	4.0
a_i	1.0	2.0
θ_e	3.7	3.7

Table A.1: Values for the sigmoid activation function.

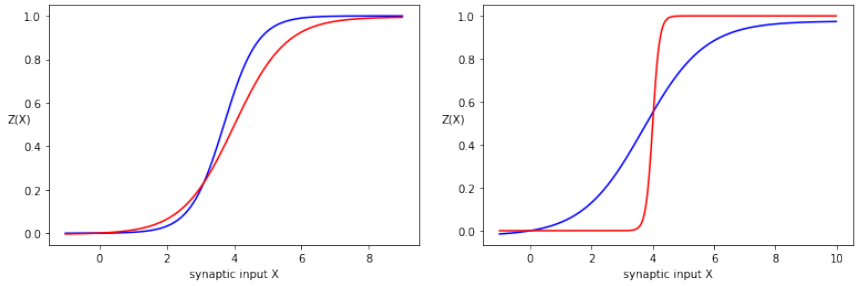

Figure A.2: The sigmoid activation functions used by Wilson-Cowan and the one we have used.

The zero values, the inverse sigmoid, the bifurnication plot Studying the isoclines is helpful for finding steady states.

To simplify the notation, E denotes the excitatory population STN and I is GPe. $\frac{dE_{STN}}{dt} = 0$ and $\frac{dI_{GPe}}{dt} = 0$

$$w_8 * I = w_9 * E - Z_e^{-1}(\frac{E}{k_e - E}) + P$$

$$w_7 * E = w_{10} * I + Z_i^{-1}(\frac{I}{k_i - I}) - Q$$

Cortex recieves a constant input, so after a some time the system reaches a steady state where $P = w_3 * E_{Cx}$ and $Q = w_1 * I_{D2}$ are constant. Z^{-1} is the inverse of the sigmoid function

$$Z_p^{-1}(x) = \theta_p - \frac{ln(\frac{1-x-y}{x-y})}{a_p}$$

$$y = \frac{-1}{1 + e^{a_p \theta_p}}$$

The nullclines can be seen in figure A.3. In the rightmost plot both the nullclines are plotted. The intersection of the two gives an equilibrium point. If there is only one such intersection and its state is unstable, limit cycles emerges.

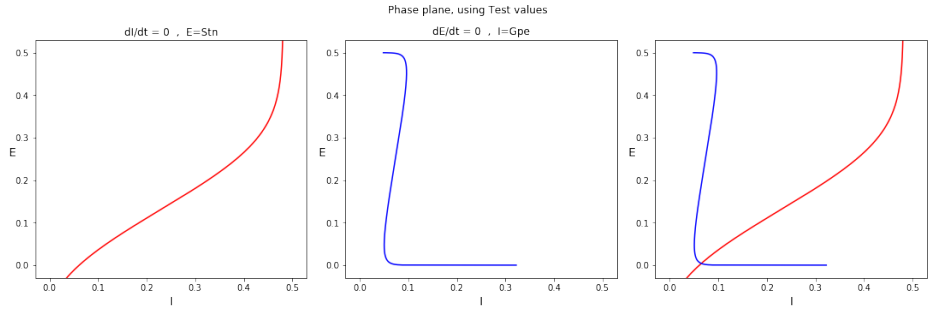

Figure A.3: The nullclines for the two populations plotted. In the rightmost plot they are plotted together, and their intersection marks an equilibrium point for the system.

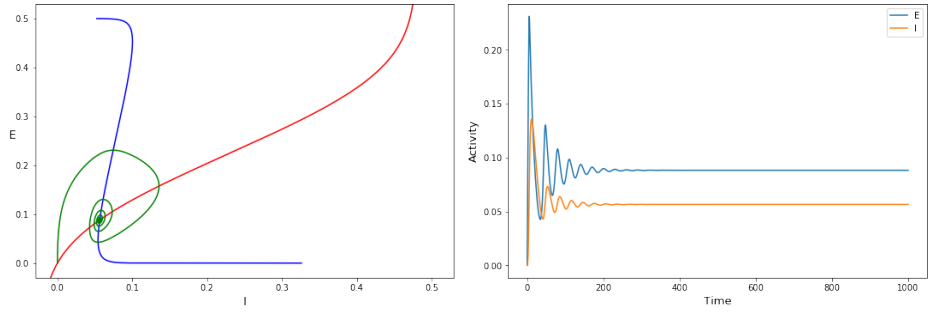

Figure A.4: Example of one phase plane . The activity of the two populations can be seen on the righthand plot, which both have damped oscillations. The activity of the populations are plotted against each other gives the green spiral in the left plot.

In models with spiking neurons, the intraconnection in the STN can be set to zero, and the basal ganglia model will still oscillate ([Mir+17]). Using this condition in our model ($w_9 = 0$) breaks with the first two of the above conditions. Adjusting the other weights by hand, we were not able to find a solution for this. We did not exhaust the possibilities of model parameters, so it is still possible that this could work. Depending on the level of activity in the cortex, oscillations could still occur in the system, however, they did not occur around the expected equilibrium point (figure A.5).

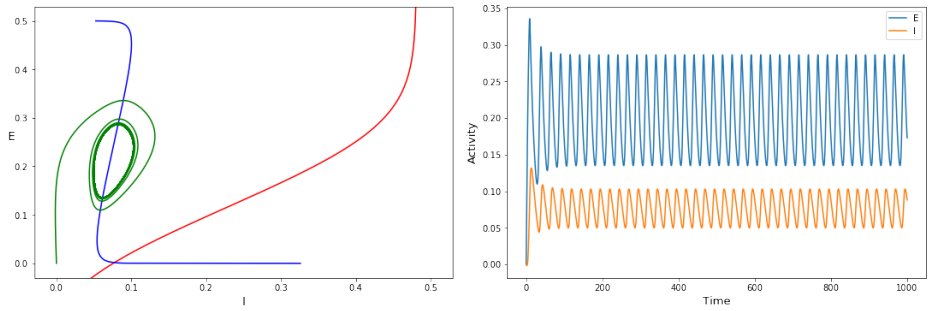

Figure A.5: Without intraconnection in the STN the model reaches a stable node, where it does not oscillate. However, when the cortex activity is changing due to thalamic feedback the system can oscillate.

Bibliography

[12] 'Extracellular spikes and CSD'. In: *Handbook of Neural Activity Measurement* (Apr. 2012), pp. 92–135.

[18] 'Multimodal modeling of neural network activity: computing LFP, ECoG, EEG and MEG signals with LFPy 2.0.' In: *Front Neuroinform* vol. 12 (2018).

[ALO16] Aspart, F., Ladenbauer, J. and Obermayer, K. 'Extending integrate-and fire model neurons to account for the effects of weak electric fields in the presence of dendrites'. In: *BMC Neuroscience* vol. 16, no. S1 (2016).

[Ant+17] Antal, A. et al. 'Low intensity transcranial electric stimulation: Safety, ethical, legal regulatory and application guidelines'. In: *Clinical Neurophysiology* vol. 128, no. 9 (2017), pp. 1774–1809.

[ARO18] Aspart, F., Remme, M. W. and Obermayer, K. 'Differential polarization of cortical pyramidal neuron dendrites through weak extracellular fields'. In: (May 2018).

[Bah+17] Bahuguna, J. et al. 'Homologous Basal Ganglia Network Models in Physiological and Parkinsonian Conditions.' In: *Frontiers in Computational Neuroscience* vol. 11 (2017).

[BAK15] Bahuguna, J., Aertsen, A. and Kumar, A. 'Existence and Control of Go/No-Go Decision Transition Threshold in the Striatum'. In: *PLOS Computational Biology* vol. 11, no. 4 (2015).

[BB13] Brittain, J.-S. and Brown, P. 'The many roads to tremor'. In: *Experimental Neurology* vol. 250 (2013), pp. 104–107.

[Bie+09] Biel, M. et al. 'Hyperpolarization-Activated Cation Channels: From Genes to Function'. In: *Physiological Reviews* vol. 89, no. 3 (2009), pp. 847–885.

[BKD06] Bédard, C., Kröger, H. and Destexhe, A. 'Model of low-pass filtering of local field potentials in brain tissue'. In: *Physical Review E* vol. 73, no. 5 (2006).

[BKD18] Bédard, C., Kröger, H. and Destexhe, A. 'Model of low-pass filtering of local field potentials in brain tissue, Revised version'. In: *Physical Review E* vol. 73, no. 5 (July 2018).

[Bri+13] Brittain, J.-S. et al. 'Tremor Suppression by Rhythmic Transcranial Current Stimulation'. In: *Current Biology* vol. 23, no. 5 (2013), pp. 436–440.

[Bro+01] Brown, P. et al. 'Dopamine Dependency of Oscillations between Subthalamic Nucleus and Pallidum in Parkinson's Disease'. In: *The Journal of Neuroscience* vol. 21, no. 3 (2001), pp. 1033–1038.

[Bro07] Brown, P. 'Abnormal oscillatory synchronisation in the motor system leads to impaired movement'. In: *Current Opinion in Neurobiology* vol. 17, no. 6 (2007), pp. 656–664.

[Cag+14] Cagnan, H. et al. 'The nature of tremor circuits in parkinsonian and essential tremor'. In: *Brain* vol. 137, no. 12 (Aug. 2014), pp. 3223–3234.

[Cag+16] Cagnan, H. et al. 'Stimulating at the right time: phase-specific deep brain stimulation'. In: *Brain* vol. 140, no. 1 (2016), pp. 132–145.

[Cag+19] Cagnan, H. et al. 'Publisher Correction: Emerging technologies for improved deep brain stimulation'. In: *Nature Biotechnology* vol. 37, no. 10 (Sept. 2019), pp. 1237–1237.

[Cog+16] Cogan, S. F. et al. 'Tissue Damage Thresholds during Therapeutic Electrical Stimulation.' In: *Journal of Neural Engineering* vol. 13, no. 2 (Apr. 2016), p. 021001.

[Dmo+17] Dmochowski, J. P. et al. 'Optimal use of EEG recordings to target active brain areas with transcranial electrical stimulation'. In: *NeuroImage* vol. 157 (2017), pp. 69–80.

[ECB12] Eusebio, A., Cagnan, H. and Brown, P. 'Does suppression of oscillatory synchronisation mediate some of the therapeutic effects of DBS in patients with Parkinsons disease?' In: *Frontiers in Integrative Neuroscience* vol. 6 (2012).

[GR16] Goldwyn, J. H. and Rinzel, J. 'Neuronal coupling by endogenous electric fields: cable theory and applications to coincidence detector neurons in the auditory brain stem'. In: *Journal of Neurophysiology* vol. 115, no. 4 (Jan. 2016), pp. 2033–2051.

[Gro+17] Grossman, N. et al. 'Noninvasive Deep Brain Stimulation via Temporally Interfering Fields.' In: *Cell*, no. 169 (June 2017), pp. 1029–1041.

[Hal+12] Hallermann, S. et al. 'State and location dependence of action potential metabolic cost in cortical pyramidal neurons'. In: *Nature Neuroscience* vol. 15, no. 7 (Mar. 2012), pp. 1007–1014.

[Hol+18] Holt, A. B. et al. 'Phase-Dependent Suppression of Beta Oscillations in Parkinsons Disease Patients'. In: *The Journal of Neuroscience* vol. 39, no. 6 (2018), pp. 1119–1134.

[Kol06] Kole, M. H. P. 'Single Ih Channels in Pyramidal Neuron Dendrites: Properties, Distribution, and Impact on Action Potential Output'. In: *Journal of Neuroscience* vol. 26, no. 6 (Aug. 2006), pp. 1677–1687.

[Kum+11] Kumar, A. et al. 'The Role of Inhibition in Generating and Controlling Parkinson?s Disease Oscillations in the Basal Ganglia'. In: *Frontiers in Systems Neuroscience* vol. 5 (2011).

[LB12] Little, S. and Brown, P. 'What brain signals are suitable for feedback control of deep brain stimulation in Parkinsons disease?' In: *Annals of the New York Academy of Sciences* vol. 1265, no. 1 (2012), pp. 9–24.

[LB14] Little, S. and Brown, P. 'The functional role of beta oscillations in Parkinsons disease'. In: *Parkinsonism Related Disorders* vol. 20 (2014).

[Lit+13] Little, S. et al. 'Adaptive deep brain stimulation in advanced Parkinson disease'. In: *Annals of Neurology* vol. 74, no. 3 (Dec. 2013), pp. 449–457.

[LJ06] Lai, H. C. and Jan, L. Y. 'The distribution and targeting of neuronal voltage-gated ion channels'. In: *Nature Reviews Neuroscience* vol. 7, no. 7 (2006), pp. 548–562.

[LPE10] Lindén, H., Pettersen, K. H. and Einevoll, G. T. 'Intrinsic dendritic filtering gives low-pass power spectra of local field potentials'. In: *Journal of Computational Neuroscience* vol. 29, no. 3 (2010), pp. 423–444.

[Mak+19] Maki-Marttunen, T. et al. 'Biophysical Psychiatry: How Computational Neuroscience Can Help to Understand the Complex Mechanisms of Mental Disorders'. In: *Frontiers in Psychiatry* vol. 10 (2019).

[Mal+12] Mallet, N. et al. 'Dichotomous Organization of the External Globus Pallidus'. In: *Neuron* vol. 74, no. 6 (2012), pp. 1075–1086.

[Mir+17] Mirzaei, A. et al. 'Sensorimotor Processing in the Basal Ganglia Leads to Transient Beta Oscillations during Behavior'. In: *The Journal of Neuroscience* vol. 37, no. 46 (2017), pp. 11220–11232.

[Næs+17] Næss, S. et al. 'Corrected Four-Sphere Head Model for EEG Signals'. In: *Frontiers in Human Neuroscience* vol. 11 (2017).

[NB98] Nowak, L. G. and Bullier, J. 'Axons, but not cell bodies, are activated by electrical stimulation in cortical gray matter'. In: *Experimental Brain Research* vol. 118, no. 4 (1998), pp. 477–488.

[Nes+15] Ness, T. et al. 'Modelling and Analysis of Electrical Potentials Recorded in Microelectrode Arrays (MEAs).' In: *Neuroinformatics* vol. 13, no. 4 (2015), pp. 403–426.

[NRE18] Ness, T. V., Remme, M. W. and Einevoll, G. T. 'h-Type Membrane Current Shapes the Local Field Potential from Populations of Pyramidal Neurons'. In: *The Journal of Neuroscience* vol. 38, no. 26 (June 2018), pp. 6011–6024.

[NRS18] Nejad, M. M., Rotter, S. and Schmidt, R. 'Transmission of motor signals from the basal ganglia to the thalamus: effect of correlations, sensory responses, and excitation'. In: (2018).

[Ros+14] Rosenbaum, R. et al. 'Axonal and synaptic failure suppress the transfer of firing rate oscillations, synchrony and information during high frequency deep brain stimulation'. In: *Neurobiology of Disease* vol. 62 (2014), pp. 86–99.

[Ste14] Sterratt, D. *Principles of computational modelling in neuroscience*. Cambridge University Press, 2014.

[WC72] Wilson, H. R. and Cowan, J. D. 'Excitatory and Inhibitory Interactions in Localized Populations of Model Neurons'. In: *Biophysical Journal* vol. 12, no. 1 (1972), pp. 1–24.

[Wes+18] West, T. O. et al. 'Propagation of beta/gamma rhythms in the cortico-basal ganglia circuits of the parkinsonian rat'. In: *Journal of Neurophysiology* vol. 119, no. 5 (Jan. 2018), pp. 1608–1628.

[You+17] Yousif, N. et al. 'A Network Model of Local Field Potential Activity in Essential Tremor and the Impact of Deep Brain Stimulation'. In: *PLOS Computational Biology* vol. 13, no. 1 (Sept. 2017).

[You+20] Yousif, N. et al. 'A Population Model of Deep Brain Stimulation in Movement Disorders From Circuits to Cells'. In: *Frontiers in Human Neuroscience* vol. 14 (May 2020).